

SEMI-ANALYTICAL MODELS FOR THE FORMATION OF DISK GALAXIES – II. DARK MATTER VERSUS MODIFIED NEWTONIAN DYNAMICS

FRANK C. VAN DEN BOSCH¹ AND JULIANNE J. DALCANTON
Department of Astronomy, University of Washington, Seattle, WA 98195, USA
(vdbosch,jd)@astro.washington.edu
Submitted for publication in ApJ

ABSTRACT

We present detailed semi-analytical models for the formation of disk galaxies both in a Universe dominated by dark matter (DM), and in one for which the force law is given by modified Newtonian dynamics (MOND). We tune the models to fit the observed near-infrared Tully-Fisher (TF) relation, and compare numerous predictions of the resulting models with observations. The DM and MOND models are almost indistinguishable. They both yield gas mass fractions and dynamical mass-to-light ratios which are in good agreement with observations. Both models reproduce the narrow relation between global mass-to-light ratio and central surface brightness, and reveal a characteristic acceleration, contrary to claims that these relations are not predicted by DM models. Both models require SN feedback in order to reproduce the lack of high surface brightness dwarf galaxies. However, the introduction of feedback to the MOND models steepens the TF relation and increases the scatter, making MOND only marginally consistent with observations. The most serious problem for the DM models is their prediction of steep central rotation curves. However, the DM rotation curves are only slightly steeper than those of MOND, and are only marginally inconsistent with the poor resolution data on LSB galaxies.

Subject headings: galaxies: formation — galaxies: fundamental parameters — galaxies: spiral — galaxies: kinematics and dynamics — galaxies: structure — dark matter.

1. INTRODUCTION

The most successful cosmological model to date consists of a universe dominated by cold dark matter (CDM), possibly with a non-zero cosmological constant. However, this paradigm faces several serious shortcomings. First is the high central densities predicted for virialized dark halos. Navarro, Frenk & White (1996, 1997) have claimed the existence of a universal density profile for virialized halos, with $\rho_{\text{DM}} \propto r^{-1}$ at small radii (hereafter referred to as the NFW profile). More recently, higher resolution simulations have argued that CDM halos should have even steeper cusps (Fukushige & Makino 1997; Moore et al. 1998; Moore et al. 1999b; but see Kravtsov et al. 1998). Several studies have argued that these steep cusps are inconsistent with the observed rotation curves of dark matter dominated systems, such as dwarfs and low surface brightness galaxies (Flores & Primack 1994; Moore 1994; Burkert 1995; Navarro 1998; McGaugh & de Blok 1998a; Stil 1999). Secondly, Klypin et al. (1999) and Moore et al. (1999a) have indicated an additional problem for the CDM paradigm: simulations predict that galaxies should have many more satellite systems than observed. Although the reason for this large discrepancy may be related to observational biases, feedback from supernovae, or an ionizing background, it might also indicate that the CDM power spectrum has too much power on small scales. Both these problems may (partially) be solved with a mixture of hot and cold dark matter. However, the dark matter scenario is certainly starting to lose its appealing character, if we have to rely on a hybrid mix of baryons, cold dark matter, hot dark matter, and a non-zero cosmological constant in order to explain the observations. The problems with fine-tuning become more and more severe, and

it might therefore be worthwhile to explore some alternatives to the dark matter theory.

Although the flat rotation curves of galaxies are generally interpreted as evidence for the existence of dark matter, they could also result from our theory of gravity (or inertia) being in error, such that the dynamical masses inferred from the usual Newtonian equations are overestimated. Several groups have tried to eliminate the need for dark matter by modifying the theory of gravity (e.g., Milgrom 1983a; Sanders 1986; Mannheim & Kazanas 1989; Liboff 1992; Moffat & Sokolov 1996). So far, the modified Newtonian dynamics (MOND) proposed by Milgrom (1983a) has been remarkably successful, and in this paper we compare several predictions from MOND with those based on dark matter (hereafter DM).

Disk galaxies are, from a dynamical point of view, fairly simple systems in which the discrepancies between the luminous and the inferred dynamical masses (the “mass discrepancies”) are least ambiguous. In addition, they have been extensively studied, with data available for systems that span several orders of magnitude in both mass and surface brightness. They are thus the ideal test-beds to compare predictions based on MOND and DM with observations in the hope to discriminate between the two alternatives.

For both MOND and DM to be considered viable theories, they should be able to explain the following properties of disk galaxies:

1. The slope, scatter, and zero-point of the Tully-Fisher relation (Tully & Fisher 1977). In particular, the fact that both high and low surface brightness disks (HSBs and LSBs, respectively) follow the same re-

¹Hubble Fellow

lation without any significant offset (Sprayberry et al. 1995; Zwaan et al. 1995; Hoffman et al. 1996; Tully & Verheijen 1997).

2. The shape of the observed rotation curves. In particular, the systematic variation of these curves with surface brightness and luminosity (Rubin, Thonnard & Ford 1980; Burstein et al. 1982; Casertano & van Gorkum 1991; Persic, Salucci & Stel 1996).
3. The increase of mass discrepancies with decreasing luminosity and surface brightness (e.g., Salucci & Frenk 1989; Persic & Salucci 1988, 1990; Kormendy 1990; Broeils 1992; Forbes 1992; Persic, Salucci & Stel 1996; McGaugh & de Blok 1998a). This is directly linked to item 2.
4. The increase of gas mass fractions with decreasing luminosity and surface brightness (Gavazzi 1993; Gavazzi, Pierini & Boselli 1996; McGaugh & de Blok 1997).
5. The sharp cut-off in the distribution of central surface brightnesses at the bright end, close to the value of the Freeman (1970) law (Allen & Shu 1979; McGaugh, Bothun & Schombert 1995; de Jong 1996a; McGaugh & de Blok 1998a).
6. The presence of a characteristic acceleration in the rotation curves of disk galaxies (McGaugh 1998).

In a series of papers, McGaugh & de Blok (1998a,b; hereafter MB98a and MB98b) have used several of these observational facts to argue against the DM hypothesis and in favor of MOND. In particular, they argue that the DM hypothesis faces severe fine-tuning problems. In this paper we revisit these issues using more sophisticated models for the formation of disk galaxies under both the DM and MOND hypotheses. We show that, contrary to the claims made by MB98a and MB98b, the DM model can explain virtually all aforementioned observations with a minimal amount of fine-tuning. Furthermore, we show that MOND needs a similar amount of fine-tuning, thereby losing its apparent advantage over the DM scenario.

This paper is organized as follows. In §2 we discuss the models, both for the DM and the MOND models. In §3 we use the near-infrared Tully-Fisher relation to constrain the free parameters of the models. In §4 we compare the models to data on gas mass fractions, dynamical mass-to-light ratios, and characteristic accelerations. §5 compares the detailed rotation curve shapes from the DM and MOND models. We summarize our conclusions in §6. Throughout this paper we adopt a Hubble constant of $H_0 = 70 h_{70} \text{ km s}^{-1} \text{ Mpc}^{-1}$ in all our models. Any quantity that depends on the distance scale is written in terms of h_{70} .

2. THE FORMATION OF DISK GALAXIES

2.1. The dark matter hypothesis

In van den Bosch (1999; hereafter Paper I) we presented detailed models for the formation of disk galaxies in the context of a universe dominated by CDM. Here we briefly summarize the ingredients of the models, and refer the reader to Paper I for details.

In our models, disks form by the settling of baryonic matter in virialized dark halos, which are described by the NFW density profile. We assume that while the baryons radiate their binding energy, they conserve their specific angular momentum, thus settling into a disk with a scale length that is proportional to the angular momentum and size of the dark halo (see also Fall & Efstathiou 1980; Dalcanton Spergel & Summers 1997; Mo, Mao & White 1998; van den Bosch 1998). The angular momentum, J , is thought to originate from cosmological torques and can be characterized by a dimensionless spin parameter, λ , the distribution of which is well constrained from both analytical and numerical studies (e.g., Barnes & Efstathiou 1987; Warren et al. 1992). For each separate model galaxy, we randomly draw a value for λ from this distribution. The disk is assumed to be a thin exponential with surface density $\Sigma(R) = \Sigma_0 \exp(-R/R_d)$. Adiabatic contraction is taken into account to describe how the density profile of the dark matter changes due to the cooling of the baryonic matter (Blumenthal et al. 1986; Flores et al. 1993). A global stability criterion is used to investigate if the disks that form are stable. If unstable, part of the disk material is transformed into a bulge component, until the disk reaches stability (van den Bosch 1998).

Once the density distribution of the baryonic material is known, we compute the fraction of baryons converted into stars. Kennicutt (1989) has shown that the star formation rate (SFR) in disk galaxies follows a Schmidt law (Schmidt 1959), but is abruptly suppressed below a given threshold density. The critical density is given by Toomre's (1964) stability criterion as:

$$\Sigma_{\text{crit}}(R) = \frac{\sigma_{\text{gas}} \kappa(R)}{3.36 G Q} \quad (1)$$

Here Q is a dimensionless constant near unity, σ_{gas} is the velocity dispersion of the gas, and κ is the epicycle frequency, which can be derived from the rotation curve.

Setting $\sigma_{\text{gas}} = 6 \text{ km s}^{-1}$ and $Q = 1.5$ these star formation thresholds were found to coincide with the radii where $\Sigma_{\text{gas}} = \Sigma_{\text{crit}}$. Following an earlier suggestion by Quirk (1972), we therefore consider the fraction of disk mass with surface densities in excess of Σ_{crit} to be eligible for star formation. If one further considers the empirical Schmidt law determined by Kennicutt (1998) for a large sample of disk galaxies, it is found that over the typical lifetime of a galaxy virtually all the mass which is eligible for star formation does in fact turn into stars. This is consistent with the lack of major star formation in the inter-arm regions in spirals and yields gas mass fractions that are in good agreement with observations (Paper I). In what follows we therefore assume that the entire bulge mass and the entire disk mass with $\Sigma(R) > \Sigma_{\text{crit}}$ are transformed into stars, giving a total stellar mass of M_* .

The total K -band luminosity of the disk-bulge system is then calculated using $L_K = M_*/\Upsilon_K^*$, where Υ_K^* is the stellar mass-to-light ratio. Since Υ_K^* depends only weakly on the age and metallicity of a stellar population (see discussion in Paper I), we assume a constant stellar mass-to-light ratio of $\Upsilon_K^* = 0.4 h_{70} \text{ M}_\odot / L_\odot$.

With the mass in stars known, the total amount of energy produced by SN can be calculated, once we make assumptions about the energy per SN (E_{SN}) and the number of SN per solar mass of stars formed (η_{SN}). We then

calculate the total baryonic mass that is prevented from becoming part of the disk/bulge system due to SN feedback as

$$M_{\text{hot}} = 3.22 M_* \varepsilon_{\text{SN}}^0 \times \left(\frac{\eta_{\text{SN}}}{0.004 M_\odot^{-1}} \right) \left(\frac{E_{\text{SN}}}{10^{51} \text{erg}} \right) \left(\frac{V_{200}}{250 \text{ km s}^{-1}} \right)^{\nu-2}. \quad (2)$$

Here V_{200} corresponds to the circular velocity of the halo at the radius r_{200} , inside of which the average density equals 200 times the critical density for closure, and $\varepsilon_{\text{SN}}^0$ and ν are two free parameters that describe the efficiency with which the SN energy is used to prevent gas from settling in the disk/bulge system (see Paper I). Throughout we adopt a value of $\eta_{\text{SN}} = 0.004 M_\odot^{-1}$ which corresponds to a Scalo (1986) initial mass function. An iterative procedure is used to compute the masses in the various phases in a self-consistent manner, i.e., we ensure that $M_{200} = M_{\text{DM}} + M_* + M_{\text{cold}} + M_{\text{hot}}$, with M_{200} the total mass within r_{200} (before SN blow-out), and M_{cold} the disk mass that is not turned into stars.

2.2. The modified Newtonian dynamics hypothesis

We now construct similar models but under the hypothesis of MOND, which assumes that the force law changes from conventional Newtonian form when the acceleration of a test particle is smaller than a characteristic acceleration a_0 (which is a universal constant). The true gravitational acceleration \mathbf{a} is related to the Newtonian acceleration \mathbf{a}_N as

$$\mu(a/a_0) \mathbf{a} = \mathbf{a}_N \quad (3)$$

($a = |\mathbf{a}|$). The interpolation function $\mu(x)$ is not specific, but is required to have the asymptotic behavior $\mu(x \gg 1) \rightarrow 1$ (the Newtonian regime) and $\mu(x \ll 1) \rightarrow x$ (the MOND regime). With the rotation law given as usual, $V_c^2(r)/r = a$, the circular velocity of a finite bounded mass M in the limit $a \rightarrow 0$ becomes

$$V_\infty = (G M a_0)^{1/4}, \quad (4)$$

with G the gravitational constant. MOND thus predicts asymptotically flat rotation curves.

First we need to set a_0 and the interpolation function $\mu(x)$. We follow previous studies of MOND, and set $a_0 = 1.12 \times 10^{-10} h_{70} \text{ ms}^{-2}$ and adopt

$$\mu(x) = \frac{x}{\sqrt{1+x^2}}. \quad (5)$$

For these choices, MOND yields good fits to the observed rotation curves of disk galaxies (Kent 1987; Milgrom 1988; Begeman, Broeils & Sanders 1991; Sanders 1996; de Blok & McGaugh 1988). With $\mu(x)$ given by equation (5), the circular velocity as function of radius becomes

$$V_c(r) = V_N(r) \left[\frac{1}{2} + \sqrt{\frac{1}{4} + \frac{a_0^2 r^2}{V_N^4(r)}} \right]^{1/4}, \quad (6)$$

where $V_N(r) = \sqrt{r d\Phi/dr}$ is the circular velocity derived for pure Newtonian dynamics.

Unfortunately, there is currently no MOND equivalent to the theory of structure formation in a DM universe.

In particular, we don't know the formation epochs or distribution of angular momenta of galaxies that form in a MOND universe. We therefore follow an empirical procedure in which we assume that galaxy formation under MOND produces disk galaxies with the masses and dimensions as observed. As in the DM scenario, disks are assumed to be thin exponentials. We randomly draw a total (baryonic) mass from the interval $10^8 h_{70}^{-1} M_\odot \leq M_{\text{tot}} \leq 5.7 \times 10^{11} h_{70}^{-1} M_\odot$. We initially set the disk mass, M_d , equal to M_{tot} , and randomly draw a central disk surface density from the interval $45 h_{70} M_\odot \text{pc}^{-2} \leq \Sigma_0 \leq 2400 h_{70} M_\odot \text{pc}^{-2}$. The scale length of the disk is then $R_d = (M_d/2\pi\Sigma_0)^{1/2}$.

The first step is to investigate whether the disk is stable against global instabilities. To that extent we use the same stability criterion as for the DM scenario, i.e., a disk is considered stable if

$$\alpha = 0.3 \frac{\sqrt{G M_d/R_d}}{V_c(3R_d)} < \alpha_{\text{crit}}, \quad (7)$$

where $V_c(3R_d)$ is the circular velocity of the galaxy at three scale lengths (cf. Christodolou, Shlosman & Tohline 1995; Efstathiou, Lake & Negroponte 1982; van den Bosch 1998). In the case of Newtonian dynamics with no DM halos, $\alpha = 0.5$. However, in the case of MOND, $\alpha < 0.5$, at least if the acceleration at $3R_d$ is sufficiently small; i.e., the MOND force law helps to stabilize disks (Milgrom 1989). Unlike the DM scenario, for which numerical simulations have shown that $\alpha_{\text{crit}} \simeq 0.35$ (Christodolou et al. 1995), no equivalent study exists based upon MOND. We therefore consider α_{crit} a free parameter.

Once the density distribution of the gas is known, we calculate the mass in stars, in the same fashion as for the dark matter models discussed above. Note, however, that in the calculation of the epicycle frequency, κ , we now use the circular velocity based on the modified force law. The K -band luminosity is again calculated from M_* adopting a constant mass-to-light ratio Υ_K^* , which we consider a free parameter.

Finally, we include SN feedback, using the same approach as above for DM. The hot gas mass, M_{hot} is calculated using equation (2), but with V_{200} replaced by V_∞ (equation [4]). We use an iterative technique to ensure self-consistency, i.e., $M_{\text{tot}} = M_* + M_{\text{cold}} + M_{\text{hot}}$.

3. CONSTRAINTS FROM THE TULLY-FISHER RELATION

The slope, scatter and zero-point of the Tully-Fisher (hereafter TF) relation contain information about the structure and formation of disk galaxies. Here we use the observed characteristics of this fundamental scaling relation to set the parameters of our disk formation models described in the previous section.

3.1. Observations and simple dynamical predictions

The slope and scatter of the empirical TF relation depend strongly on the luminosity and velocity measures used, with the relation becoming shallower going towards bluer passbands (Aaronson, Huchra & Mould 1979; Visvanathan 1981; Tully, Mould & Aaronson 1982; Wyse 1982; Pierce & Tully 1988; Gavazzi 1993; Verheijen 1997). Therefore, when trying to infer constraints on the structure and formation of disk galaxies from the TF relation, it

is absolutely essential that one extracts the same luminosity and velocity measures from the models (see discussions in Courteau 1997, Verheijen 1997, and Paper I).

The empirical TF relation which most directly reflects the mass in stars and the total dynamical mass of the halo is the K -band TF relation of Verheijen (1997), which uses the flat part of the rotation curve as a characteristic velocity:

$$L_K = 2.96 \times 10^{11} h_{70}^{-2} L_\odot \left(\frac{V_{\text{flat}}}{250 \text{ km s}^{-1}} \right)^{4.2}. \quad (8)$$

The slope of this TF relation is $b = -10.5 \pm 0.5$, and the observed scatter is $\sigma_M = 0.29$ mag. This empirical TF relation is shown in the upper left panel of Figure 1. Open circles correspond to the galaxies in Verheijen's sample of Ursa Major spirals, and the thick solid line is the best-fitting TF relation (equation [8]).

Within the DM framework, simple dynamics predict a TF relation of the form

$$L_K = \frac{\epsilon_{\text{gf}} f_{\text{bar}}}{10 G H_0 \Upsilon_K} \left(\frac{V_{200}}{V_{\text{flat}}} \right)^3 V_{\text{flat}}^3, \quad (9)$$

(Dalcanton et al. 1997; White 1997; Mo et al. 1998; Syer, Mao & Mo 1999; van den Bosch 1998; Paper I). Here ϵ_{gf} is the galaxy formation efficiency, which describes what fraction of the baryonic mass inside the DM halo ultimately ends up in the disk/bulge system, f_{bar} is the baryonic mass fraction of the Universe ($f_{\text{bar}} = \Omega_{\text{bar}}/\Omega_0$), and $\Upsilon_K = M_{\text{gal}}/L_K = \Upsilon_K^* M_{\text{gal}}/M_*$ is the K -band mass-to-light ratio of the galaxy (disk plus bulge).

From equation (4) it is immediately apparent that in the case of MOND, the TF relation becomes

$$L_K = \frac{1}{a_0 G \Upsilon_K} \left(\frac{V_\infty}{V_{\text{flat}}} \right)^4 V_{\text{flat}}^4, \quad (10)$$

(see e.g., Milgrom 1983b; MB98b).

Thus whereas DM predicts a TF relation with a slope of $b = -7.5$, MOND predicts $b = -10$, in agreement with the empirical relation of equation (8). In the case of DM, extra physics are required to steepen the predicted TF relation to the observed slope. MB98a have presented a detailed discussion in which they argue that this results in a serious fine-tuning problem for DM. On the other hand, the almost perfect agreement between the observed TF slope and the pure-gravitational value for MOND (equation [10]) presents an anti-fine-tuning problem. There is very little room for any other galaxy characteristic to vary systematically with mass, without changing the TF slope.

The above suggests that simple dynamical arguments can be used to predict the existence of an underlying TF relation for both DM and MOND. However, to accurately predict the slope, zero-point, and scatter of the TF relationship, it is necessary to incorporate the more detailed physics discussed in §2. We do so in the following two sections for the DM and MOND hypotheses, respectively. As mentioned in §3.1 it is essential to extract the same velocity measure from the models as the one used in the data, and we therefore extract V_{flat} from our model galaxies (see paper I for details).

3.2. The Tully-Fisher relation and dark matter

In Paper I we showed that taking the stability-derived star formation threshold densities into account (with $Q = 1.5$) steepens the TF relation from $L_K \propto V_{\text{flat}}^3$ (as predicted by pure dynamics) to $L_K \propto V_{\text{flat}}^{3.6}$. We argued that to further steepen the TF relation to its observed slope, feedback from SN is required. Fine-tuning the two parameters that describe the efficiency with which SN energy is used to prevent gas from settling in the disk/bulge system (ϵ_{SN}^0 and ν), we were able to obtain a TF relation with a slope, zero-point, and an amount of scatter that are all in excellent agreement with the empirical relation of equation (8). This model is referred to as model L5 in Paper I, and we adopt the same convention here. This model is based on a cosmology with $\Omega_0 = 0.3$, $\Omega_\Lambda = 0.7$, $h_{70} = 1$ and $\sigma_8 = 1.0$ (see paper I), and its parameters are listed in Table 1. Model L5 predicts an intrinsic TF scatter of $\sigma_M \simeq 0.2$ mag, with no offset in normalization between HSB and LSB galaxies, as observed. The TF relation of model L5 is shown in the upper right panel of Figure 1.

3.3. The Tully-Fisher relation and MOND

Although simple dynamics predict a TF relation for MOND with a slope $b = -10$, consistent with observations, this ignores the fact that Υ_K varies with mass; gas mass fractions are known to increase with decreasing mass (see §4.2), and taking this into account steepens the TF relation. It therefore remains to be seen whether MOND does not actually predict TF relations that are too steep. We can investigate this using the models described in §2.2.

As with the DM models, we set $Q = 1.5$. The stellar mass-to-light ratio in the K -band, Υ_K^* , is set by fitting the normalization of the TF relation, yielding $\Upsilon_K^* = 0.53 h_{70} M_\odot / L_\odot$. This value is consistent with estimates based on stellar population models, which in itself can be considered a success of MOND.

To set the free parameter α_{crit} , with the help of equation (6) the stability criterion (equation [7]) can be written as

$$\Sigma_0 \leq 1.91 \times 10^3 \left(\frac{a_0}{10^{-10} \text{ m s}^{-2}} \right) \times \left[\left(\frac{1}{8 \alpha_{\text{crit}}^4} - 1 \right)^2 - 1 \right]^{-1/2} M_\odot \text{ pc}^{-2}. \quad (11)$$

The stability parameter α_{crit} thus directly translates into a maximum surface density of disks. From the fact that the brightest observed disks have central surface brightnesses of $\mu_{0,K} \simeq 16.5$ mag arcsec $^{-2}$ (e.g., de Jong 1996b; Tully et al. 1996) we infer $\alpha_{\text{crit}} \gtrsim 0.45$ (for $\Upsilon_K^* = 0.53 h_{70} M_\odot / L_\odot$). If we were to take $\alpha_{\text{crit}} = 0.35$ (as for the DM models), no disks with central surface brightnesses brighter than $\mu_{0,K} = 18.1$ mag arcsec $^{-2}$ would be allowed, clearly inconsistent with observations. Since in general not all the gas mass is transformed into stars, the limit of $\alpha_{\text{crit}} = 0.45$ is conservative. We find that with $Q = 1.5$ and $\Upsilon_K^* = 0.53 h_{70} M_\odot / L_\odot$ a value of $\alpha_{\text{crit}} = 0.48$ yields $\mu_{0,K} \lesssim 16.5$ mag arcsec $^{-2}$, and we adopt this value throughout. None of the results presented here, however, depend on this choice: α_{crit} merely sets the maximum central surface density for disks with a given bulge-to-disk ratio, and is set such that we obtain disks with the full range of observed

values of $\mu_{0,K}$. In mimicking the sample selection of Verheijen (1997) we only consider model galaxies with a bulge-to-disk ratio $B/D \leq 0.2$ (see also Paper I).

We compare the DM model (L5) with two different MOND models, M1 and M2. The former neglects SN feedback, whereas the latter considers blow-out by SN with $\varepsilon_{\text{SN}}^0 = 0.05$ and $\nu = -3.0$ (see Table 1). The motivation for these particular feedback parameters will be discussed in §4.3. The TF relations for models M1 and M2 are shown in the lower panels of Figure 1. The star formation recipe with $Q = 1.5$ steepens the MOND TF relation from $L_K \propto V_{\text{flat}}^4$ (equation [10]) to $L_K \propto V_{\text{flat}}^{4.2}$ (model M1), and brings it in excellent agreement with the empirical TF relation of Verheijen. The predicted, intrinsic amount of scatter is only $\sigma_M = 0.21$ mag, once again in excellent agreement with observations. The introduction of SN feedback steepens the TF relation further, to $b = -11.9$ for model M2, and increases the scatter to $\sigma_M = 0.33$ mag. Model M2 thus yields a TF relation that is too steep. In addition, the amount of scatter is only marginally consistent with the data, i.e., Verheijen (1997) derived $\sigma_M \leq 0.3$ mag at 95 percent confidence level.

4. COMPARISON OF MODELS WITH DATA

Having tuned the parameters by fitting the near-infrared TF relation, we now compare the resulting models to other independent observations, to test, amongst others, the validity of the star formation and feedback recipes used. As shown in paper I, within the CDM context one can construct many physically different models that all fit the empirical TF relation. For these models additional constraints, such as the ones described below, are required to discriminate between the models.

4.1. The data

Our calculations yield magnitudes and surface brightnesses in the K -band and rotation velocities for a collection of model galaxies. Ideally, we would therefore compare our models to data that consists of K -band photometry combined with full HI rotation curves. Unfortunately, such data is currently scarce, and we therefore use B -band photometry, for which ample data is available. Although a constant stellar mass-to-light ratio is a reasonable assumption for the K -band, Υ_B^* is expected to reveal a systematic trend with mass as well as a significant amount of scatter owing to variations in dust content, and the ages and metallicities of the stellar populations. We convert the K -band luminosities and surface brightnesses of our model galaxies to the B -band adopting an empirically determined $B-K$ color magnitude relation (see Appendix A). This, at least, takes account of the systematic trend of $B-K$ with M_K . Unfortunately, the scatter is relatively large, and we predict errors in M_B and $\mu_{0,B}$, owing to the color conversion, of 0.37 and 0.47 mag, respectively. A more detailed comparison of our models against data has to await accurate near-infrared photometry of a large sample of disk galaxies for which full HI rotation curves are available.

We compiled the following data for comparison with our models:

- M_K , $\mu_{0,K}$, R_d , and V_{flat} for a sample of spirals in the Ursa Major cluster from the thesis of Verheijen (1997). We restrict ourselves to the twenty-two

galaxies of the “unperturbed sample” on which the TF relation of equation (8) is based. As for our models, we transform M_K and $\mu_{0,K}$ to the B -band, using the $B-K$ color magnitude relation presented in Appendix A. Data from this sample are plotted as open circles.

- M_B , $\mu_{0,B}$, R_d , and V_{flat} for a sample of thirty-two galaxies compiled by MB98a. These data are plotted as solid circles.
- M_B , $\mu_{0,B}$, R_d , and V_{max} for ten dwarf galaxies from the sample of van Zee et al. (1997). The velocity measure V_{max} is virtually identical to the velocity at the last measured point of the HI rotation curves, and as such compatible with the velocity measure determined in our models (see paper I). These data are plotted as solid squares.
- M_B , $\mu_{0,B}$, and M_{HI}/L_B for a sample of one hundred disk galaxies of type Sb or later, compiled by McGaugh & de Blok (1997). These data are plotted as open squares.

All data have been converted to $h_{70} = 1$, using the distance scales quoted by the various authors. Note that this combined set of data is by no means complete nor homogeneous. In compiling the data we have aimed for a maximum coverage in both luminosity and surface brightness of disk galaxies with measured HI rotation curves. Therefore, it is important to keep in mind that upon comparing models to data, one should only focus on global properties, such as the areas of parameter space occupied by the data and the models. Our models are not constructed to correctly predict the local density distribution of data points in parameter space (i.e., the masses of our model galaxies are sampled uniformly rather than from a Press-Schechter formalism or a luminosity function). In addition, the incompleteness and possible observational biases in the data samples, combined with the errors associated with the conversion of K -band models to the B -band, prevents us from testing our models in too much detail.

4.2. Gas mass fractions

One of the empirical characteristics of disk galaxies is the increase of their gas mass fractions with decreasing luminosity and surface brightness (i.e., item 4 in §1). This is shown in the upper left panels of Figures 2 and 3, where we plot the logarithm of the HI mass-to-light ratio, M_{HI}/L_B , as function of M_B and $\mu_{0,B}$, respectively. The remaining panels plot the results for each of the three models. The solid lines in Figures 2 and 3 have no physical meaning, but are plotted to facilitate a comparison of the models with the data.

The increase of M_{HI}/L_B with decreasing magnitude and surface brightness is remarkably well reproduced by each of the three models. Note also that the range spanned by the model galaxies is in good agreement with the data. The HI mass-to-light ratios derived from the models scale with h_{70} , whereas the measured ratios are independent of distance (the HI mass is computed directly from the observed flux). The main parameter in the models that sets M_{HI}/L_B is the star formation parameter Q . It is reassuring that for $H_0 = 70 \text{ km s}^{-1} \text{ Mpc}^{-1}$ and for the value of Q

that was empirically determined by Kennicutt (1989), the models yield gas mass fractions that are in good agreement with observations.

4.3. Dynamical mass-to-light ratios.

Dynamical mass-to-light ratios are seen to vary systematically with mass and surface brightness. Dwarfs and LSB galaxies have consistently higher mass-to-light ratios than bright HSB galaxies. These mass-to-light ratios are higher than can be explained by differences in stellar populations alone, and indicate an increasing “mass discrepancy” with decreasing luminosity and surface brightness (i.e., item 3 in §1).

In this paper we define a characteristic mass-to-light ratio²

$$\Upsilon_0 = \frac{R_d V_{\text{flat}}^2 / G}{L_B}. \quad (12)$$

In Figure 4 we plot $\log(\Upsilon_0)$ as function of M_B for the data and our three models. The thin line is plotted to facilitate a comparison, and is chosen to roughly outline the region that reveals a clear deficit of galaxies; low luminosity galaxies always have high mass-discrepancies, whereas bright disk galaxies can have values of Υ_0 that span over an order of magnitude. This absence of faint galaxies with low mass discrepancies is well reproduced by model L5, and owes largely to the effect of SN feedback. The efficiency with which SNe can blow gas out of a dark halo is larger in less massive galaxies. This causes most of the baryonic mass to be expelled from low-mass halos, resulting in higher values of Υ_0 for fainter galaxies. A possible shortcoming of model L5 seems to be the fact that it predicts virtually no galaxies with $\Upsilon_0 \lesssim 0.8$, whereas four of the sixty-four galaxies in the combined data set have values of Υ_0 below this value. However, given the scatter in the $B - K$ color magnitude relation, the inhomogeneous nature of our comparison sample, and the typical errors associated with the data, this apparent deficit is not significant.

In the MOND model without feedback (model M1), there is no reason for fainter galaxies to have systematically higher values of Υ_0 . Indeed model M1 does not reproduce the observed absence of dwarf galaxies with low mass discrepancies, and it does a poor job in reproducing the data. We therefore included feedback, and tuned the parameters $\varepsilon_{\text{SN}}^0$ and ν such that the observed ‘region of avoidance’ is reproduced, yielding model M2. Note that model M2 predicts, similarly to model L5, an absence of model galaxies with $\Upsilon_0 \lesssim 0.8$.

A similar result is shown in Figure 5, where we plot the B -band central surface brightness versus V_{flat} . The data reveal a clear absence of HSB disk galaxies with low rotation velocities. In other words, disk galaxies with $V_{\text{flat}} \lesssim 50 \text{ km s}^{-1}$ always have low surface brightness. Again, our DM model reproduces this behavior remarkably well. Model M1 predicts no such deficit, and is in clear conflict with the data. Model M2, however, in which the two SN parameters have been tuned to yield the observed absence of dwarf galaxies with low mass discrepancies, is in excellent agreement with the data.

Note that the observed regions of avoidance in both the

$M_B - \Upsilon_0$ and the $V_{\text{flat}} - \mu_{0,B}$ planes are not due to observational biases: There is no reason why dwarf galaxies with high central surface brightnesses should be missed, whereas their LSB counterparts are not (except for a possible problem due to star-galaxy separation for compact systems at large distances). This therefore seems to be a strong indication that SN feedback plays an important role in the formation of (disk) galaxies, at least for the less massive ones.

MB98a have shown that Υ_0 is strongly correlated with central surface brightness. This is confirmed from our combined data set (which includes the data of MB98a) plotted in the upper left panel of Figure 6. The thin solid line corresponds to $\Upsilon_0^2 \propto 1/\Sigma_0^*$, and is plotted with arbitrary normalization for comparison. Here Σ_0^* is the central surface brightness of the luminous, stellar disk in L_{\odot}/pc^2 . The data clearly indicates that $\Upsilon_0^2 \Sigma_0^* \sim \text{constant}$ with only little scatter.

MB98a and MB98b argue that this $\Upsilon_0 - \Sigma_0$ “conspiracy” follows naturally from MOND, whereas it requires a problematic fine-tuning in the case of DM. As shown by Zwaan et al. (1995), $\Upsilon_0^2 \Sigma_0^* = \text{constant}$ is required to obtain a TF relation in which HSB and LSB galaxies follow the same relation with a slope of $b = -10$. MB98a discuss a number of physical processes that may lead to the observed $\Upsilon_0 - \Sigma_0$ “conspiracy” under the hypothesis of DM, none of which they render feasible. The upper right panel of Figure 6, however, shows that our DM model reproduces the observed “conspiracy” to a good degree of accuracy. Given that the same model yields a TF relation with a slope close to -10 and with little scatter, this is not too surprising, since the $\Upsilon_0 - \Sigma_0$ conspiracy and the TF relation are closely connected (see discussions in Zwaan et al. 1995 and MB98a). We thus disagree with MB98a, and conclude that the $\Upsilon_0 - \Sigma_0$ relation is in fact fairly easily reproduced.

The lower two panels of Figure 6 show that the two MOND models are also in good agreement with the data, something which is not too surprising given that pure MOND dynamics predict that $\Upsilon_0^2 \propto 1/\Sigma_0^*$ (MB98b).

4.4. Characteristic accelerations

Milgrom (1983b) defined the characteristic acceleration parameter

$$\xi \equiv \frac{V_{\text{flat}}^2}{a_0 R_d}, \quad (13)$$

which is proportional to the ratio of the characteristic acceleration V_{flat}^2/R_d of a disk and the characteristic MOND acceleration a_0 . As shown by MB98b, for an exponential disk MOND predicts a tight correlation between ξ and surface brightness of the form $\xi \propto \Sigma_0^{1/2}$. The upper left panel of Figure 7 plots $\log(\xi)$ as function of $\mu_{0,B}$ for the data. The thin solid line corresponds to $\xi \propto \Sigma_0^{1/2}$, and is plotted with an arbitrary normalization. Clearly, the data reveals a narrow correlation between ξ and central surface brightness, with a slope close to that predicted by MOND. MB98b considered this yet another success of modified Newtonian dynamics.

However, as we show in Appendix B, the dark matter hypothesis predicts the same relation, i.e., $\xi \propto \Sigma_0^{1/2}$, and

²MB98a defined Υ_0 as the global mass-to-light ratio inside four disk scale lengths. If we assume that $V_c(4 R_d) \simeq V_{\text{flat}}$ and that disks are pure exponentials, our definition of Υ_0 is identical to that of MB98a, apart from a factor 0.23.

the observed relation between ξ and $\mu_{0,B}$ thus does not provide a useful test to discriminate between the MOND and DM hypotheses. This is also evident from Figure 7, which shows that each of our three models yields a relation between ξ and $\mu_{0,B}$ that is in excellent agreement with the observations. It is important, though, to note that under the DM hypothesis, the amount of scatter can be significantly larger than observed. It is because of the SN feedback, the efficiency of which decreases with increasing halo mass, that the amount of scatter in model L5 is as small as it is (see Appendix B for a detailed discussion).

Additional support for MOND was recently presented by McGaugh (1998), who showed that current observations hint to the presence of a characteristic acceleration, the main assumption on which MOND is based. The upper panels of Figure 8 plot data, kindly provided by Stacy McGaugh, of the cumulative mass discrepancy Υ against radius R (panels on the right), against orbital frequency $\omega = V_{\text{rot}}/R$ (middle panels), and against centripetal acceleration $\alpha \equiv V_{\text{rot}}^2/R$ (panels on the right). Here Υ is defined as

$$\Upsilon(R) = \frac{R V_{\text{rot}}^2(R)}{G[M_*(R) + M_{\text{cold}}(R)]}, \quad (14)$$

and corresponds to the ratio of total mass (based on the Newtonian equations) to luminous mass (stars plus cold gas) within radius R . Each data point represents one resolved measurement in the rotation curve of a disk galaxy. The galaxies in the sample span a wide range in luminosities and surface brightnesses and were taken from the compilation of Sanders (1996) and de Blok & McGaugh (1998).

The plot of Υ versus R reveals that the mass discrepancy sets in at a wide range of different radii; individual rotation curves are easily discerned. This scatter is reduced when plotting Υ versus the circular frequency, and becomes minimal when plotted versus the acceleration α . The data clearly reveal that in each disk galaxy, the mass discrepancy starts to become significant below an acceleration of $\sim 10^{-10} \text{ m s}^{-2}$, as predicted by MOND.

The lower two rows of panels of Figure 8 show the same plots for the two MOND models. Here we have randomly selected 40 galaxies from models M1 and M2, and for each model galaxy, we computed Υ at 15 radii, sampled uniformly between $R = 0$ and the radius at which the projected HI column density is equal to 10^{20} cm^{-2} . The two MOND models reproduce the data extremely well, which is to be expected, given the presence of the characteristic acceleration a_0 and the fact that MOND was specifically designed to fit rotation curves. More remarkably, model L5 also yields a characteristic acceleration (see panels in second row of Figure 8). Although the agreement with the data is not quite as good as in the case of models M1 and M2, the main characteristic of the data, namely the minimization of scatter when Υ is plotted versus α , is reproduced well. Most importantly, this is achieved without any fine-tuning of our model; after setting the feedback parameters to fit the slope of the empirical TF relation, the same model reveals a characteristic acceleration. This is in clear contradiction with McGaugh (1998), who argued that this phenomenology can not be reproduced with DM models. Not only is this a remarkable success of our DM

model, it is also an argument against an argument in favor of MOND.

Model L5 predicts mass discrepancies which are slightly too large in the range $3 \times 10^9 \lesssim \alpha \lesssim 10^{10} \text{ m s}^{-2}$. The origin of this small deficit is discussed in the following §.

4.5. Understanding the scaling relations

Why can our DM models easily account for the Υ_0 - Σ_0 “conspiracy”, whereas MB98a have argued that no feasible solution exists? Combining equations [12] and [13], and taking into account that the total luminosity of an exponential disk scales as $L \propto \Sigma_0 R_d^2$, one obtains $\Upsilon_0 \propto \xi \Sigma_0^{-1}$. Since, as shown in Appendix B, we have $\xi \propto \Sigma_0^{1/2}$ one thus automatically predicts that $\Upsilon_0 \propto \Sigma_0^{-1/2}$; i.e., *there is no conspiracy*. However, the fact that the scatter around the Υ_0 - Σ_0 relation is so small is not trivial, as the scatter in the ξ - Σ_0 relation can be fairly large. It is only because of our particular feedback model, which we tuned to reproduce the empirical TF relation, that the scatter in the ξ - Σ_0 relation, and therewith in the Υ_0 - Σ_0 relation, is so small (see Appendix B). We consider this another major success for our feedback model.

From the scaling relations listed above one derives that $\xi \propto \Upsilon_0^{-1}$. We thus expect a narrow correlation between the characteristic accelerations and mass-to-light ratios of disk galaxies. Therefore, the fact that our DM model is successful in reproducing the narrow correlation between *local* accelerations and mass-to-light ratios is not too surprising.

5. ROTATION CURVE SHAPES

The rotation curves (hereafter RCs) of disk galaxies are the most direct indicators of a discrepancy between the luminous mass and the inferred dynamical mass for disk galaxies. The shapes of rotation curves therefore provide a clean laboratory for comparing models of gravitational dynamics. Historically, astronomers have explained the detailed RCs of spiral galaxies by invoking the presence of non-luminous matter (see reviews in Sancisi & van Albada 1987, and Ashman 1992), while preserving the r^{-2} force law of Newtonian gravity. More recently, some astronomers have used MOND to explain the observed kinematics without requiring the presence of dark matter (e.g. Kent 1987; Lake 1989; Begeman et al. 1991; Sanders 1996; de Blok & McGaugh 1998; Sanders & Verheijen 1998). Both approaches have found nearly equal success over a wide range of luminosities and surface brightnesses, well beyond the luminous, high-surface brightness galaxies for which the theories of DM and MOND were developed.

Recently, an important problem for the CDM picture has emerged from HI studies of dwarf galaxies. The slowly rising rotation curves observed in these systems suggest a (close to) constant density core in their dark matter halos, inconsistent with the steeply cusped density profiles predicted for CDM (Flores & Primack 1994; Moore 1994; Burkert 1995; Burkert & Silk 1997; Stil 1999, but see Kravtsov et al. 1998). Whether MOND is consistent with the RCs of dwarf galaxies, is an issue that is currently still under debate (Lake 1989; Milgrom 1991; Sánchez-Salcedo & Hidalgo-Gómez 1999).

Recent studies have shown that more massive LSB disk galaxies reveal rotation curves that are similar to those of

dwarf galaxies (e.g., de Blok, McGaugh & van der Hulst 1996; van Zee et al. 1997; Pickering et al. 1997), suggesting that the problem with the density profiles of dark matter halos is not limited to low-mass systems. Indeed, MB98a have argued that the observed rotation curve of LSB galaxies are inconsistent with the NFW profile. MOND, however, has been shown to yield remarkably good fits to the RCs of LSB galaxies (de Blok & McGaugh 1998; Sanders & Verheijen 1998). It is important to note, however, that the majority of the data on the RCs of the more massive LSB galaxies is severely affected by beam smearing (see e.g., Swaters 1999). Van den Bosch, Robertson & Dalcanton (1999) have shown that once these effects are taken into account, the RCs of the more massive LSB galaxies are in excellent agreement with dark matter halos with steep central cusps.

5.1. A detailed comparison

Given the unique opportunity to discriminate between DM and MOND based on the RC shapes of disk galaxies, we now compare the RCs predicted by our DM and MOND models in some detail. Using our models which best fit the K -band TF relation (L5 and M1), we have selected model galaxies that are photometrically similar (same scale length, same absolute magnitude, and same central surface brightness), and computed their RCs. In Figure 9 we compare four sets of model galaxies that span four magnitudes in both surface brightness and mass (see Table 2 for the parameters of each of the eight galaxies).

For the high surface brightness galaxies, (d1, m1, d3, and m3) the RCs for the MOND and the DM models are very similar. For the LSB galaxies, however, the galaxies from the DM model predict RCs that are significantly steeper in the inner parts. This is the reason why dark halo fits to several LSB galaxies have been claimed to fail, and owes to the steep central cusp (r^{-1} for the NFW profile used in our DM models) of the dark halo. This also explains why $\Upsilon(R)$ is slightly overestimated for accelerations at around $3 \times 10^9 \lesssim \alpha \lesssim 10^{10} \text{ m s}^{-2}$ (see Figure 8) as compared to the observations. Note, however, that the data on which Figure 8 is based suffers strongly from the beam-smearing effects eluded to above, and it remains to be seen whether it is actually inconsistent with the predictions from our DM model (see van den Bosch et al. 1999).

The steepness of the central part of the RCs can be quantified by the parameter $R_{3/4}$, which is defined as the radius at which the circular velocity equals 75 percent of V_{flat} . MB98a obtained $R_{3/4}$ for a number of disk galaxies with reasonably well resolved HI rotation curves, and found $R_{3/4}/R_d$ to strongly increase with decreasing luminosity and surface brightness. They compared this to predictions based on the models of Dalcanton et al. (1997; hereafter DSS97), which are similar to the models presented here. According to MB98a, the models of DSS97 predict an opposite behavior from that observed, with $R_{3/4}/R_d$ decreasing with decreasing magnitude, and they use this as strong evidence against DM models.

To further test this, we compute $R_{3/4}/R_d$ for the model galaxies in each of our three models. Results are plotted as function of M_B and $\mu_{0,B}$ in Figure 10. The first characteristic to notice is that none of the models reveals a significant increase of $R_{3/4}/R_d$ with decreasing magnitude. The MOND models reveal a modest increase of $R_{3/4}/R_d$

with decreasing surface brightness, but they reach a maximum at $R_{3/4} \simeq 1.25R_d$. The galaxies of model L5 never reach values of $R_{3/4}/R_d$ in excess of ~ 0.8 . Both models are therewith in clear contradiction with the observed RCs presented by MB98a, which reach values as high as $R_{3/4}/R_d \sim 3$. The most likely explanation for this discrepancy is, once again, beam smearing, which tends to over-predict $R_{3/4}/R_d$ (see e.g., Blais-Ouellette, Carignan & Amram 1998). Data of higher spatial resolution is required to test this further. However, given the modest difference between the predictions from MOND and the DM models, it seems unlikely that $R_{3/4}/R_d$ will allow to discriminate between the two scenarios

Not only are the results presented here inconsistent with data, they also disagree with the curves plotted by MB98a which they claim to represent the model predictions from DSS97. However, we do not understand how MB98a have obtained these predictions. Part of the answer may lie in the fact that MB98a quote that they used models with $L \propto \Sigma_0^{1/3}$ “as predicted by DSS97”. However, the models of DSS97 predict $\Sigma_0 \propto L^{1/3}$. Nevertheless, even with this erroneous interpretation of DSS97’s models, we are unable to reproduce the predictions of MB98a. The results presented here suggest that neither MOND nor the DM hypothesis predict a strong dependence of $R_{3/4}/R_d$ on either luminosity or surface brightness. Together with the fact that the MOND and DM models yield results that differ only modestly, we conclude that they both are equally (in)consistent with the data. The observed values of $R_{3/4}/R_d$ can not be used to simply rule against the DM hypothesis only.

6. CONCLUSIONS

We have presented detailed models for the formation of disk galaxies in both a CDM and a MOND universe. In the case of DM, the structure of the disk is governed by the mass and angular momentum of the proto-galaxy. For MOND, however, the distribution of angular momenta of proto-galaxies is not known, and we have instead assigned scale lengths to the disks that are in agreement with observations. In addition to these recipes that determine the structure and dynamics of the disks, we include recipes that describe how (part of) the gas is transformed into stars over the lifetime of the galaxy. We take account of a stability related threshold density for star formation and feedback from supernovae. The models have been tuned to fit the observed K -band TF relation, and compared to numerous observations. Both models do remarkably well in reproducing a wide variety of observations of disk galaxies that span several orders of magnitude in both luminosity and surface brightness.

To more easily compare the different models a summary of the results is given in Table 3, where we indicate, for each of the observational constraints discussed in this paper, whether the models are consistent with the data or not. In the case of DM (model L5), SN feedback is required to yield a TF slope as steep as observed. Although the MOND model without feedback (M1) is in excellent agreement with the empirical TF relation, it does not reproduce the observed deficit of HSB dwarf galaxies with small mass-discrepancies. This can be remedied by introducing SN feedback (model M2), but at the cost of a TF

relation which is too steep and reveals an amount of scatter that is only marginally consistent with the data. This is a serious problem for MOND; since pure dynamics already predicts a TF relation as steep as observed, it leaves virtually no room for any other galaxy characteristics to vary systematically with mass.

The DM model is consistent with all observational constraints against which we have tested it. Consequently, we strongly disagree with the picture that emerges from the literature (for example, MB98a, MB98b, and McGaugh 1998), that the DM hypothesis suffers from numerous serious fine-tuning problems, which do not seem to have a clear-cut solution, whereas MOND is free from such problems and capable of fitting virtually everything. We have shown here that once the DM model is tuned to fit the slope of the TF relation, it automatically passes all the tests devised by MB98a and McGaugh (1998) to argue against it. In particular, our DM model reproduces

- A close correlation between global mass-to-light ratio and surface brightness, such that HSB and LSB galaxies follow the same TF relation without a systematic offset.
- The presence of a characteristic acceleration as observed.
- A close relation between the characteristic acceleration, ξ , and central surface brightness of the form $\xi \propto \Sigma_0^{-0.2}$.

This is a remarkable result: there is no obvious reason why the DM model would reveal a characteristic acceleration, unlike in the case of MOND, where it is integral to the theory. Furthermore, it is encouraging that the same feedback parameters that yield the correct TF slope, result in an amount of scatter around the ξ - Σ_0 relation that is in excellent agreement with observations, and in addition explains the observed absence of HSB dwarfs with small mass-discrepancies.

Of the list of observational facts about disk galaxies presented in §1, the upper limit to the observed surface brightness of disk galaxies (item 5) has not been addressed by our models. Several studies have shown, however, that in the DM picture the presence of a maximum central surface brightness of disk galaxies is related to stability arguments (DSS97; Mo et al. 1998; Scorza & van den Bosch 1998). In §3.3 we have shown that the same stability argument also yields an upper limit on the central surface brightness of disks under the hypothesis of MOND (cf. Milgrom 1989). Henceforth, both the DM and the MOND models are consistent with the observational constraint of item 5, as long as disk stability is taken into account.

The main problem for CDM is related to rotation curve shapes. We have compared predicted rotation curve shapes within the context of both MOND and CDM. Only in the case of LSB systems do the two scenarios yield RCs that are significantly different. Several studies have pointed out that dark halos with a steep cusp are inconsistent with the central rotation curves of LSB and dwarf galaxies. This problem is also evident from the fact that at accelerations of $\sim 10^{-10} h_{70} \text{ m s}^{-2}$ the DM model predicts mass-to-light ratios that are slightly too high. However, it is important to realize that most data on the more

massive LSB disks is severely affected by beam-smearing. This tends to underestimate the central gradients of rotation velocities, especially in galaxies that have a central hole in their HI distribution. When beam smearing is taken into account, the HI rotation curves of massive LSB galaxies are consistent with dark halos that follow a NFW density profile (van den Bosch et al. 1999). Further indications that beam smearing plays an important role comes from a comparison of the ratio $R_{3/4}/R_d$. Both the DM and the MOND models predict ratios that are lower than observed, which is most likely due to beam smearing. Therefore, in order to discriminate between MOND and DM, high resolution rotation curves of LSB disk galaxies are required. Such data is currently only available for dwarf galaxies, which, because of their relative proximity, have been observed with high spatial resolution. It has been demonstrated convincingly that the rotation curves of these low-mass systems are inconsistent with centrally cusped dark matter halos. It is currently still under debate whether MOND can fit these rotation curves. If it can, this is where MOND has a clear advantage over CDM, unless (close to) constant density cores can be produced in dark halos that form in a CDM Universe (see e.g., Navarro, Eke & Frenk 1996, Kravtsov et al. 1998, and Bullock et al. 1999 for possible solutions).

One might argue that within the DM scenario one can fit basically anything as long as there are a sufficient number of free parameters. In that respect it is important to realize that model L5 has only a very limited number of truly free parameters. Where possible, we have used parameters that have either empirically determined values, or that are otherwise constrained: the dark halo properties are taken from high resolution numerical simulations combined with the Press-Schechter formalism, Υ_K^* is constrained by stellar population models, the star formation recipe uses values for Q and the Schmidt law that have been determined empirically, and α_{crit} is constrained by numerical simulations. This leaves only $\varepsilon_{\text{SN}}^0$ and ν as real free parameters. Tuning these two parameters to obtain a TF relation with the observed slope of $b = -10.5$, the model predicts gas mass fractions, characteristic accelerations, an $\Upsilon_0 - \Sigma_0$ “conspiracy”, and global mass-to-light ratios which are in excellent agreement with observations, without additional tuning of the parameters. Furthermore, we note that while MOND is often presented as being nearly free of fine-tuning, in order to match the systematic properties of disk galaxies it is necessary to adjust the MOND feedback parameters to the same degree as required for DM.

Probably the most amazing aspect of the models presented here, is that the DM and MOND models are so very similar. However, both MOND and DM were constructed to fit the rotation curves of disk galaxies. The fact that both theories correctly predict many other properties, which are themselves closely related to the internal dynamics (i.e., TF relation, gas mass fractions that are set by stability related threshold densities, SN feedback whose efficiency depends on the escape velocity, etc), should therefore not be seen as too remarkable. It has often been argued that even if MOND turns out to not be correct, one should provide an explanation as to why it fits the properties of galaxies so well. The demonstrations in this paper suggest that *any* theory which yields

stable disks and fits their rotation curves, would probably perform as well as any of the models presented here.

This work has benefited greatly from discussions with George Lake. We are grateful to Stacey McGaugh for sending us his data in electronic format, and to the anonymous referee for his suggestions that helped to improve the paper. FvdB was supported by NASA through Hubble Fellowship grant # HF-01102.11-97.A awarded by the Space Telescope Science Institute, which is operated by AURA for NASA under contract NAS 5-26555.

APPENDIX

A. THE $B - K$ COLOR MAGNITUDE RELATION FOR SPIRAL GALAXIES

In order to compare our models, which yield K -band magnitudes and surface brightnesses, to B -band data, we require an estimate of $B - K$ colors for disk galaxies.

To determine an empirical $B - K$ color magnitude relation we compiled apparent magnitudes in B and K as well as distances for a total of 139 spiral galaxies of type Sb or later from the following sources: forty-two Ursa-Major spirals from the sample of Verheijen (1997), sixty-one galaxies from the sample of de Jong & van der Kruit (1994), and thirty-six galaxies from the sample of edge-on spirals of Dalcanton et al. (1999). Absolute magnitudes were computed assuming $H_0 = 70 \text{ km s}^{-1} \text{ Mpc}^{-1}$ and using the distances as quoted by these authors. Finally, we used the reddening maps of Schlegel, Finkbeiner & Davis (1998), with the $R_V = 3.1$ extinction law of Cardelli, Clayton & Mathis (1989) and O'Donnell (1994), to correct for external extinction.

The resulting $B - K$ color magnitude is shown in the upper left panel of Figure 11. The solid line is the best linear fit with

$$B - K = -0.66 - 0.18(M_K - 5 \log h_{70}). \quad (\text{A1})$$

The upper right panel plots the predicted B -band magnitude, $M_B^{\text{pred}} = 0.82 M_K^{\text{obs}} - 0.66$ versus the observed value (for $h_{70} = 1$). The data covers over eight magnitudes in M_B and reveals that M_B^{pred} is a fairly good estimate of the observed B -band magnitude (with a standard deviation of $\sigma_M = 0.37$ mag).

The lower left panel of Figure 11 plots the $B - K$ color of the central surface brightness of the disks, versus $\mu_{0,K}$ for the data of Verheijen (1997) and de Jong & van der Kruit (1994). Unfortunately, at this time no central surface brightnesses are available for the data of Dalcanton et al. (1999). Note that $B - K$ and $\mu_{0,B} - \mu_{0,K}$ are generally not the same, since the disk scale lengths derived from the B and K -band data can differ considerably (see e.g., de Jong 1996b; Verheijen 1997). The lower right panel of Figure 11 plots the predicted central surface brightness in the B -band, $\mu_{0,B}^{\text{pred}}$, versus the observed value. Here $\mu_{0,B}^{\text{pred}}$ is calculated from $\mu_{0,K}^{\text{obs}}$ and the color-magnitude relation of equation (A1). Note that the agreement is reasonable, but that the scatter is, with $\sigma_\mu = 0.47$ mag, slightly higher than for the absolute magnitudes.

B. THE CHARACTERISTIC ACCELERATION PARAMETER ξ

In §4.4 we show that both the DM and MOND models yield a narrow correlation between the central surface brightness of the disk and the parameter ξ defined by equation (13). Here we investigate the reason for this narrow relation.

In the case of MOND, $V_{\text{flat}}^4 = G a_0 M_{\text{gal}}$, and, if we assume that the galaxy is a pure exponential disk, it is straightforward to show that

$$\log(\xi_{\text{MOND}}) = -\frac{1}{5}(\mu_{0,B} - 27.052) + \frac{1}{2} \log\left(\frac{2\pi G}{a_0} \Upsilon_{\text{gal}}\right), \quad (\text{B1})$$

(see MB98b), with Υ_{gal} the total mass-to-light ratio of the galaxy.

In order to obtain a similar expression under the hypothesis of DM, we make the simplifying assumption that dark halos are represented by isothermal spheres, and that $V_{\text{flat}} = V_{200}$. Upon writing $M_d = \epsilon_{\text{gf}} f_{\text{bar}} M_{200}$ (cf. equation [9]), and since

$$M_{200} = \frac{V_{200}^3}{10 G H_0}, \quad (\text{B2})$$

we obtain

$$\xi_{\text{DM}} = \sqrt{\frac{20 \pi G H_0 V_{200} \Sigma_0}{a_0^2 \epsilon_{\text{gf}} f_{\text{bar}}}}. \quad (\text{B3})$$

If we now set $H_0 = 70 \text{ km s}^{-1}$ and $f_{\text{bar}} = 0.085$ (as for model L5, see Paper I), we can write

$$\log(\xi_{\text{DM}}) = \log(\xi_{\text{MOND}}) - 0.11 + \frac{1}{2} \log\left(\frac{V_{200}}{250 \text{ km s}^{-1}}\right) - \frac{1}{2} \log(\epsilon_{\text{gf}}). \quad (\text{B4})$$

Under the DM hypothesis one thus expects a similar relation between ξ and μ_0 as under MOND, apart from an offset which depends on V_{200} and the galaxy formation efficiency ϵ_{gf} . Since disks with the same central surface brightness can be embedded in halos with different rotation velocities (cf. Figure 5), one expects a reasonable amount of scatter; a variation in V_{200} of a factor five, yields a scatter of 0.35 in $\log(\xi)$. However, this can be significantly reduced when SN feedback is important; the feedback efficiency will be larger, leading to smaller values of ϵ_{gf} in systems with lower values of V_{200} , thus reducing the amount of scatter. Indeed, the scatter revealed by model L5 (see upper panel of Figure 7) is somewhat larger than in the case of MOND, but significantly smaller than 0.35 and therewith consistent with the data.

We thus conclude that the observed relation $\xi \propto \Sigma_0^{1/2}$ does not discriminate between the DM and the MOND hypotheses. However, the small amount of scatter observed may be considered evidence for efficient SN feedback, at least within the context of DM.

REFERENCES

- Aaranson, M., Huchra, J., & Mould, J. 1979, *ApJ*, 229, 1
- Allen, R. J., & Shu, F. H. 1979, *ApJ*, 227, 67
- Ashman, K. M. 1992, *PASP*, 104, 1109
- Barnes, J. E., & Efstathiou, G. 1987, *ApJ*, 319, 575
- Begeman, K. C., Broeils, A. H., & Sanders, R. H. 1991, *MNRAS*, 249, 523
- Blais-Ouellette, S., Carignan, C., & Amram, P. 1998, preprint (astro-ph/9811142)
- Blumenthal, G. R., Faber, S. M., Flores, R., & Primack, J. R. 1986, *ApJ*, 301, 27
- Broeils, A. H. 1992, Ph.D. Thesis, University of Groningen
- Bullock, J. S., Kolatt, T. S., Sigad, Y., Somerville, R. S., Kravtsov, A. V., Klypin, A. A., & Dekel, A. 1990, preprint (astro-ph/9908159)
- Burkert, A. 1995, *ApJ*, 447, L25
- Burkert, A., & Silk, J. 1997, *ApJ*, 488, L55
- Burstein, D., Rubin, V. C., Thonnard, N., & Ford, W. K. Jr. 1982, *ApJ*, 253, 70
- Cardelli, J. A., Clayton, G. C., & Mathis, J. S. 1989, *ApJ*, 345, 245
- Casertano, S., & van Gorkum, J. H. 1991, *AJ*, 101, 1231
- Christodoulou, D. M., Shlosman, I., & Tohline, J. E. 1995, *ApJ*, 443, 551
- Courteau, S. 1997, *AJ*, 114, 2402
- Dalcanton, J. J., Spergel, D. N., & Summers, F. J. 1997, *ApJ*, 482, 659 (DSS97)
- Dalcanton, J. J., et al. 1999, in preparation
- de Blok, W. J. G., McGaugh, S. S., & van der Hulst, J. M. 1996, *MNRAS*, 283, 18
- de Blok, W. J. G., & McGaugh, S. S. 1998, *ApJ*, 508, 132
- de Jong, R. S. 1996a, *A&A*, 313, 45
- de Jong, R. S. 1996b, *A&AS*, 118, 557
- de Jong, R. S., & van der Kruit, P. C. 1994, *A&AS*, 106, 451
- Efstathiou, G., Lake, G., & Negroponte, J. 1982, *MNRAS*, 19, 1069
- Fall, S. M., & Efstathiou, G. 1980, *MNRAS*, 193, 189
- Flores, R., Primack, J. R., Blumenthal, G. R., & Faber, S. M. 1993, *ApJ*, 412, 443
- Flores, R., & Primack, J. R. 1994, *ApJ*, 427, L1
- Forbes, D. A. 1992, *A&AS*, 92, 583
- Freeman, K. C. 1970, *ApJ*, 160, 811
- Fukushige, T., & Makino, J. 1997, *ApJ*, 477, L9
- Gavazzi, G. 1993, *ApJ*, 419, 469
- Gavazzi, G., Pierini, D., & Boselli, A. 1996, *A&A*, 312, 397
- Hoffman, G. L., Salpeter, E. E., Farhat, B., Roos, T., Williams, H., & Helou, G. 1996, *ApJS*, 105, 269
- Kent, S. M. 1987, *AJ*, 93, 816
- Kennicutt, R. C. Jr. 1989, *ApJ*, 344, 685
- Kennicutt, R. C. Jr. 1998, *ApJ*, 498, 541
- Klypin, A. A., Kravtsov, A. V., Valenzuela, O., & Prada, F. 1999, preprint (astro-ph/9901240)
- Kormendy, J. 1990, in *ASP Conf. Ser. No. 10, Evolution of the Universe of Galaxies*, ed. R. G. Kron (Provo, UT, Brigham Young University Printing Services), 109
- Kravtsov, A. V., Klypin, A. A., Bullock, J. S., & Primack, J. R. 1998, *ApJ*, 502, 48
- Lake, G. 1989, *ApJ*, 345, L17
- Liboff, R. L. 1992, *ApJ*, 397, L71
- Mannheim, P. D., & Kazanas, D. 1989, *ApJ*, 342, 635
- McGaugh, S. S. 1998, preprint (astro-ph/9812327)
- McGaugh, S. S., Bothun, G. D., & Schombert, J. M. 1995, *AJ*, 110, 573
- McGaugh, S. S., & de Blok, W. J. G. 1997, *ApJ*, 481, 689
- McGaugh, S. S., & de Blok, W. J. G. 1998a, *ApJ*, 499, 41 (MB98a)
- McGaugh, S. S., & de Blok, W. J. G. 1998b, *ApJ*, 499, 66 (MB98b)
- Milgrom, M. 1983a, *ApJ*, 270, 365
- Milgrom, M. 1983b, *ApJ*, 270, 371
- Milgrom, M. 1988, *ApJ*, 333, 689
- Milgrom, M. 1989, *ApJ*, 338, 121
- Milgrom, M. 1991, *ApJ*, 367, 490
- Mo, H. J., Mao, S., & White, S. D. M. 1998, *MNRAS*, 295, 319
- Moffat, J. W., & Sokolov, I. Yu. 1996, *Phys. Lett. B.*, 378, 59
- Moore, B., 1994, *Nature*, 370, 629
- Moore, B., Governato, F., Quinn, T., Stadel, J., & Lake, G. 1998, *ApJ*, 499, L5
- Moore, B., Ghigna, S., Governato, F., Lake, G., Quinn, T., Stadel, J., & Tozzi, P. 1999a, *Nature*, in press
- Moore, B., Quinn, T., Governato, F., Stadel, J., & Lake, G. 1999b, preprint (astro-ph/9903164)
- Navarro, J. F. 1998, preprint (astro-ph/9807084)
- Navarro, J. F., Frenk, C. S., & White, S. D. M. 1996, *ApJ*, 462, 563
- Navarro, J. F., Frenk, C. S., & White, S. D. M. 1997, *ApJ*, 490, 493
- O'Donnell, J. E. 1994, *ApJ*, 422, 1580
- Persic, M., & Salucci, P. 1988, *MNRAS*, 234, 131
- Persic, M., & Salucci, P. 1990, *MNRAS*, 245, 577
- Persic, M., Salucci, P., & Stel, F. 1996, *MNRAS*, 281, 27
- Pickering, T. E., Impey, C. D., van Gorkum, J. H., & Bothun, G. D. 1997, *AJ*, 114, 1858
- Pierce, M. J., & Tully, R. B. 1988, *ApJ*, 330, 579
- Quirk, W. J. 1972, *ApJ*, 176, L9
- Rubin, V. C., Thonnard, N., & Ford, W. K. Jr. 1980, *ApJ*, 238, 471
- Salucci, P., & Frenk, C. S. 1989, *MNRAS*, 237, 247
- Sánchez-Salcedo, F. J., & Hildalgo-Gómez, A. M. 1999, *A&A*, 345, 36
- Sancisi, R., & van Albada, T. S. 1987, in *Dark Matter in the Universe*, IAU Symp. 117, eds. J. Kormendy & G. R. Knapp (Reidel: Dordrecht), 67
- Sanders, R. H. 1986, *MNRAS*, 223, 539
- Sanders, R. H. 1996, *ApJ*, 473, 117
- Sanders, R. H. & Verheijen, M. A. W. 1998, *ApJ*, 503, 97
- Schlegel, D. J., Finkbeiner, D. P., & Davis, M. 1998, *ApJ*, 500, 525
- Schmidt, M. 1959, *ApJ*, 129, 243
- Scorza, C., & van den Bosch, F. C. 1998, *MNRAS*, 300, 469
- Sprayberry, D., Bernstein, G. M., Impey, C. D., & Bothun, G. D. 1995, *ApJ*, 438, 72
- Stil, J. 1999, Ph.D. Thesis, Leiden University
- Swaters, R. A. 1999, Ph.D. Thesis, University of Groningen
- Syer, D., Mao, S., & Mo, H. J. 1999, *MNRAS*, 305, 357
- Toomre, A. 1964, *ApJ*, 139, 1217
- Tully, R. B., & Fisher, J. R. 1977, *A&A*, 54, 661
- Tully, R. B., Mould, J., & Aaranson, M. 1982, *ApJ*, 257, 527
- Tully, R. B., Verheijen, M. A. W., Pierce, M. J., Huang, J.-S., & Wainscoat, R. J. 1996, *AJ*, 112, 2471
- Tully, R. B., & Verheijen, M. A. W. 1997, *ApJ*, 484, 145
- van den Bosch, F. C. 1998, *ApJ*, 507, 601
- van den Bosch, F. C. 1999, *ApJ*, in press (astro-ph/9909501; paper I)
- van den Bosch, F. C., Robertson, B. E., Dalcanton, J. J., & de Blok, W. J. G. 1999, *AJ*, submitted (astro-ph/9911372)
- van Zee, L., Haynes, M. P., Salzer, J. J., & Broeils, A. H. 1997, *AJ*, 113, 1618
- Verheijen, M. A. W. 1997, Ph.D. Thesis, University of Groningen
- Visvanathan, N. 1981, *A&A*, 100, L20
- Warren, M. S., Quinn, P. J., Salmon, J. K., & Zurek, W. H. 1992, *ApJ*, 399, 405
- Wyse, R. 1982, *MNRAS*, 199, 1P
- White, S. D. M. 1997, in *Galaxy Scaling Relations: Origins, Evolution and Applications*, eds. L. N. da Costa & A. Renzini (Springer-Verlag)
- Zwaan, M. A., van der Hulst, J. M., de Blok, W. J. G., & McGaugh, S. S. 1995, *MNRAS*, 273, L35

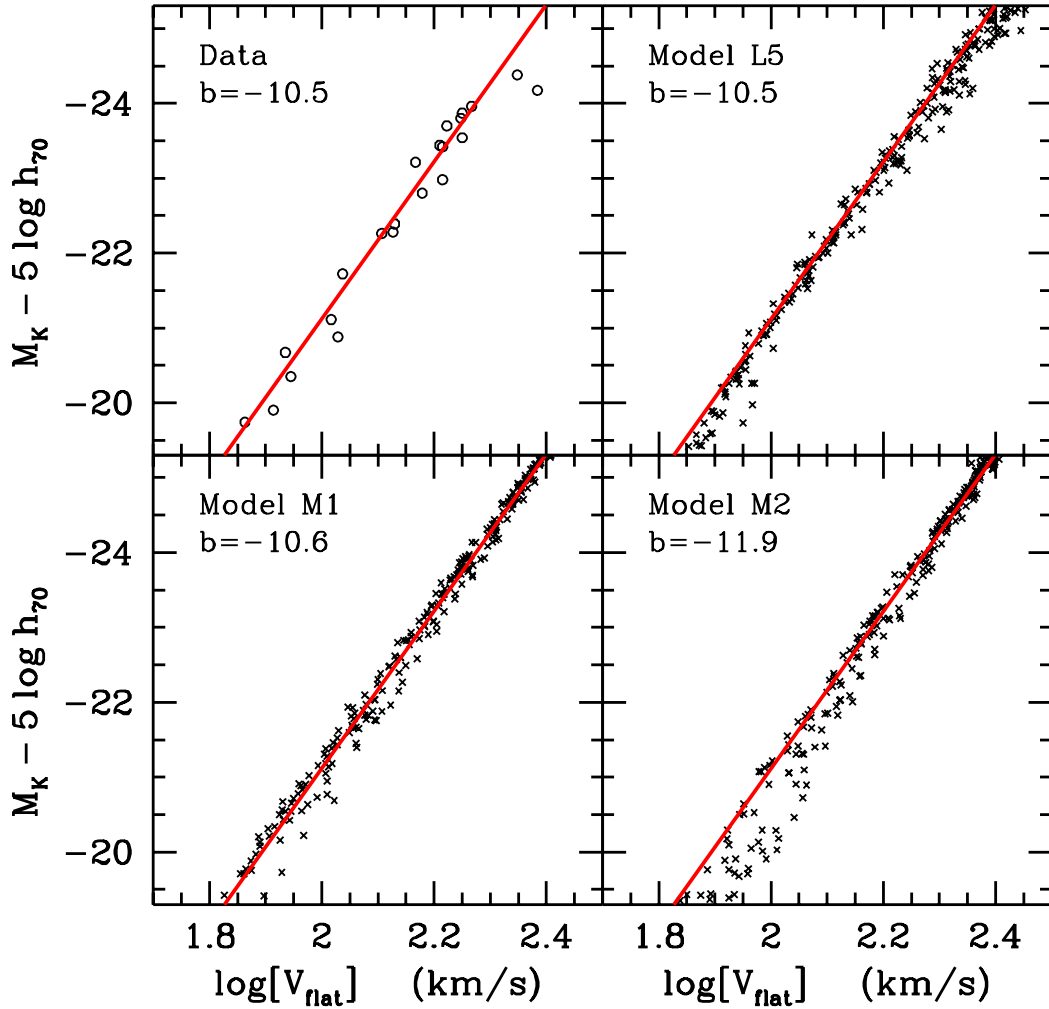


FIG. 1.— A comparison of the observed K -band TF relation with our three models. The upper left panel plots, with open circles, the twenty-two Ursa-Major spirals from the “unperturbed sample” of Verheijen (1997). The thick solid line is the best fitting TF relation (equation [8]). This line is reproduced in each of the panels. The upper right panel plots the results for our best-fitting DM model (model L5), whereas the lower two panels correspond to the two MOND models discussed in the text. The value of the slope, b , of the best-fitting TF relation is indicated in each panel.

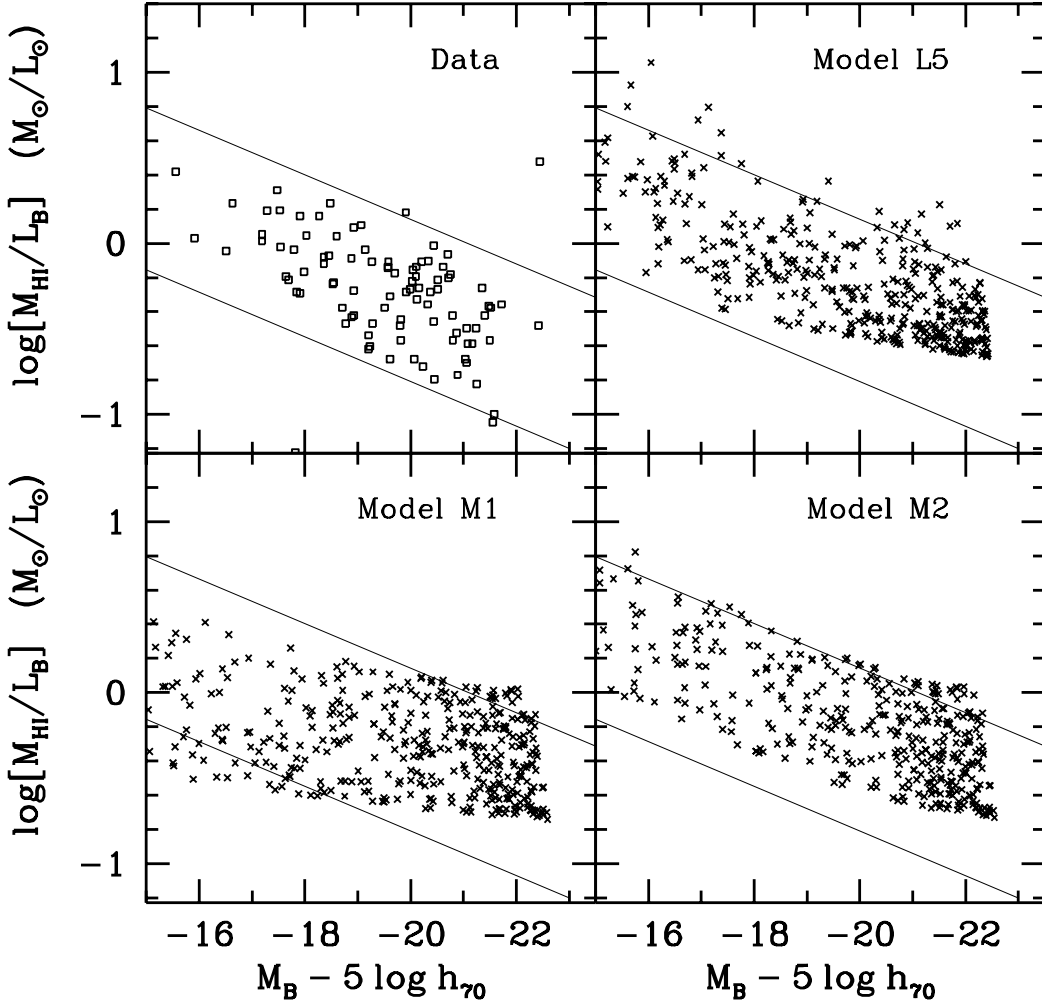


FIG. 2.— The HI mass-to-light ratios, M_{HI}/L_B , as function of total magnitude. The upper left panel plots the data for a sample of one hundred disk galaxies of type Sb or later compiled by McGaugh & de Blok (1997), and clearly reveal an increase of gas mass fractions with decreasing luminosity. The remaining three panels plot the results for each of the three models, as labeled. The two thin lines have no physical meaning, but are plotted to facilitate a comparison between models and data. Luminosities and magnitudes for the model galaxies have been converted from the K -band to the B -band using the $B-K$ color magnitude relation presented in Appendix A. Given the errorbars associated with the data, and with the color conversion, all three models are consistent with the data, and nicely reproduce the increase of M_{HI}/L_B with decreasing luminosity.

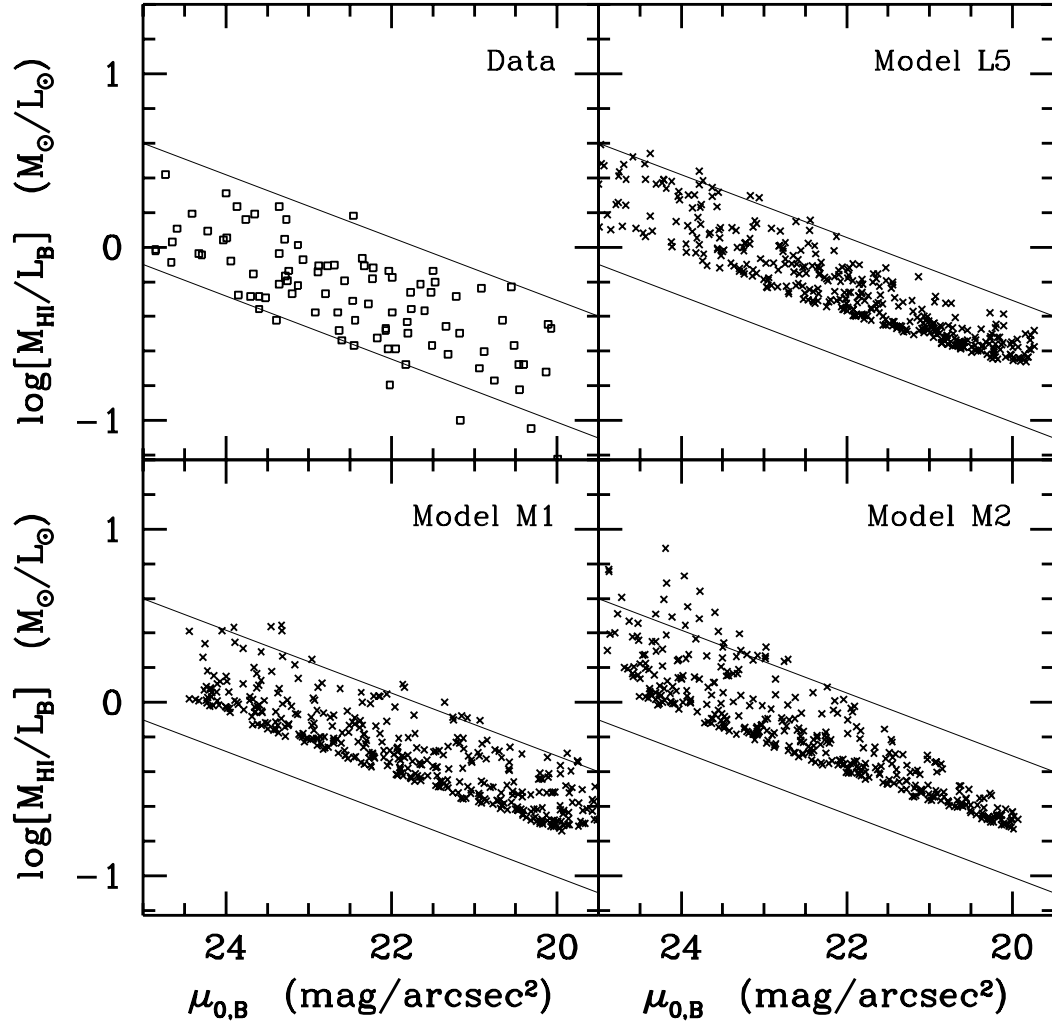


FIG. 3.— Same as Figure 2, except that now M_{HI}/L_B is plotted versus the central surface brightness of the disk, $\mu_{0,B}$. Again, the thin lines have no physical meaning but are plotted to facilitate a comparison. Clearly, the three models are all consistent with the data and with each other.

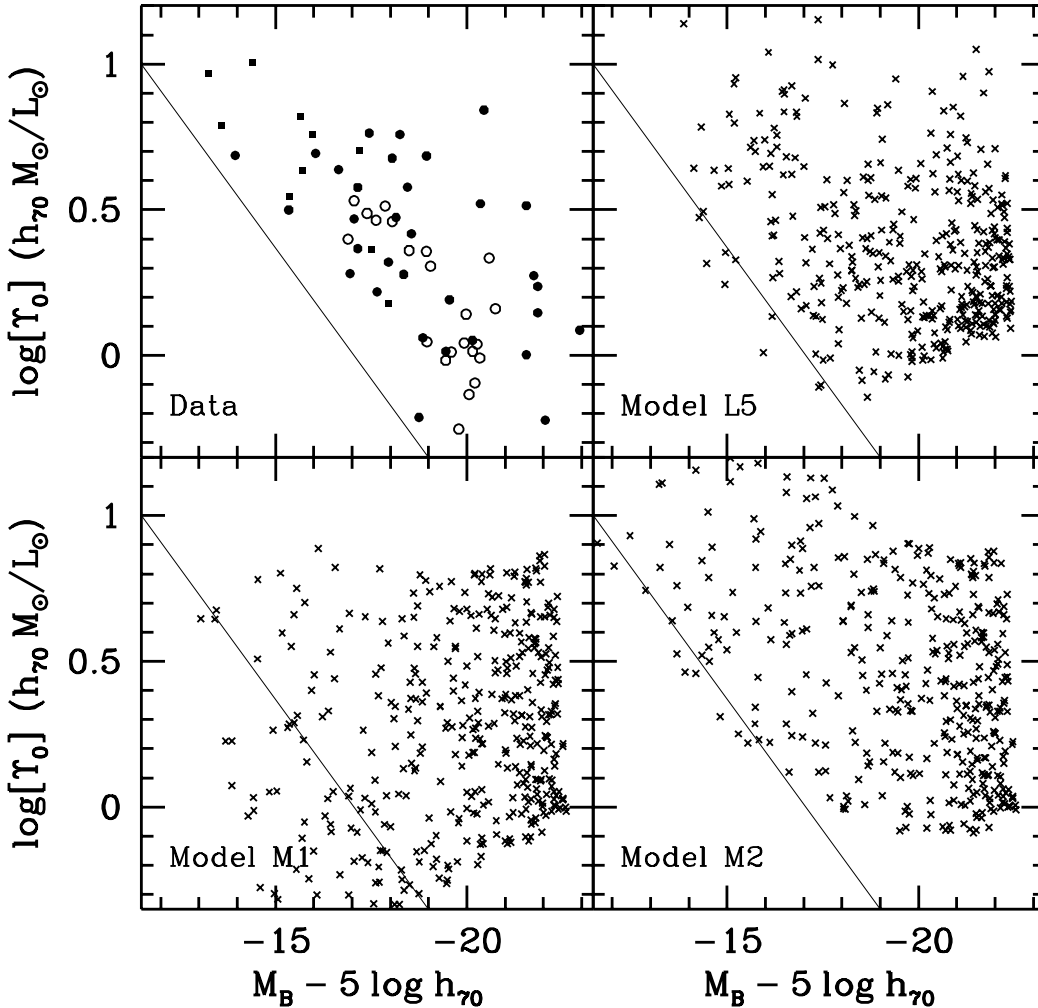


FIG. 4.— The characteristic global mass-to-light ratio Υ_0 (equation [12]) as function of absolute B -band magnitude. The data (upper left panel) are taken from Verheijen (1997; open circles), McGaugh & de Blok (1998a; solid circles), and van Zee et al. (1997; solid squares). Details on the data can be found in §4.1. The data clearly reveal an absence of faint galaxies with low values of Υ_0 , i.e., low luminosity systems always have a large mass discrepancy. This is reproduced nicely by model L5 (upper right panel), which is in reasonable agreement with the data (see the text for a more detailed discussion). Model M1, the MOND model without SN feedback, however, is clearly inconsistent with the data, in that it predicts no deficit of low luminosity systems with low values of Υ_0 . In model M2, we have included SN feedback, and tuned the corresponding parameters to reproduce the data. The thin solid line is plotted to facilitate a comparison, and is chosen to roughly outline the boundary of the data.

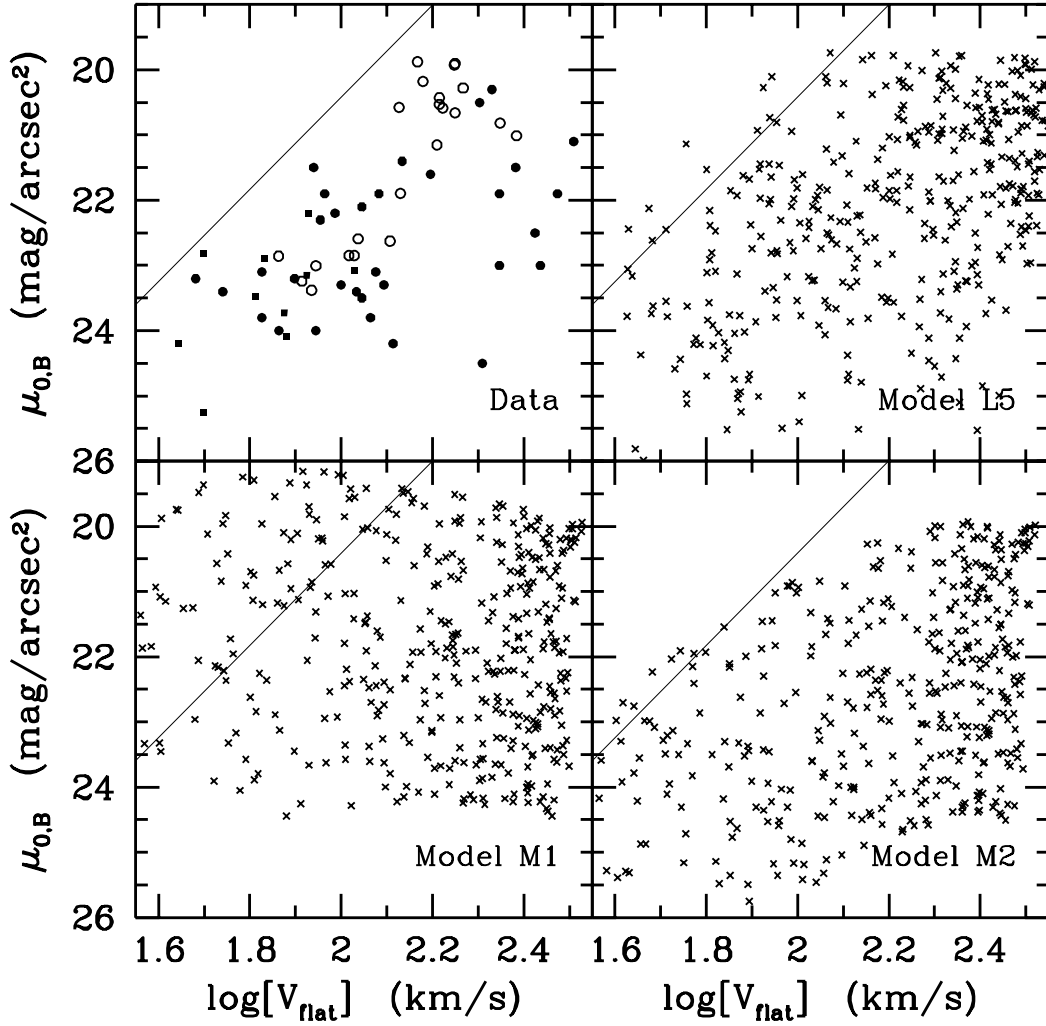


FIG. 5.— The central surface brightness of the disks ($\mu_{0,B}$) as function of the rotation velocity at the flat part of the rotation curve, V_{flat} . The symbols for the data are the same as in Figure 4. The data reveal a clear absence of HSB galaxies with low rotation velocities. This is remarkably well reproduced by models L5 and M2 (both of which include SN feedback), whereas model M1 (no SN feedback) is in clear contradiction with the data. The thin solid line is chosen to roughly outline the boundary of the data, and has no further physical meaning. Note that the absence of observed galaxies in the upper left part of the diagram is not related to observational bias effects. Rather, it seems to indicate that SN feedback has played an important role in shaping low mass disk galaxies.

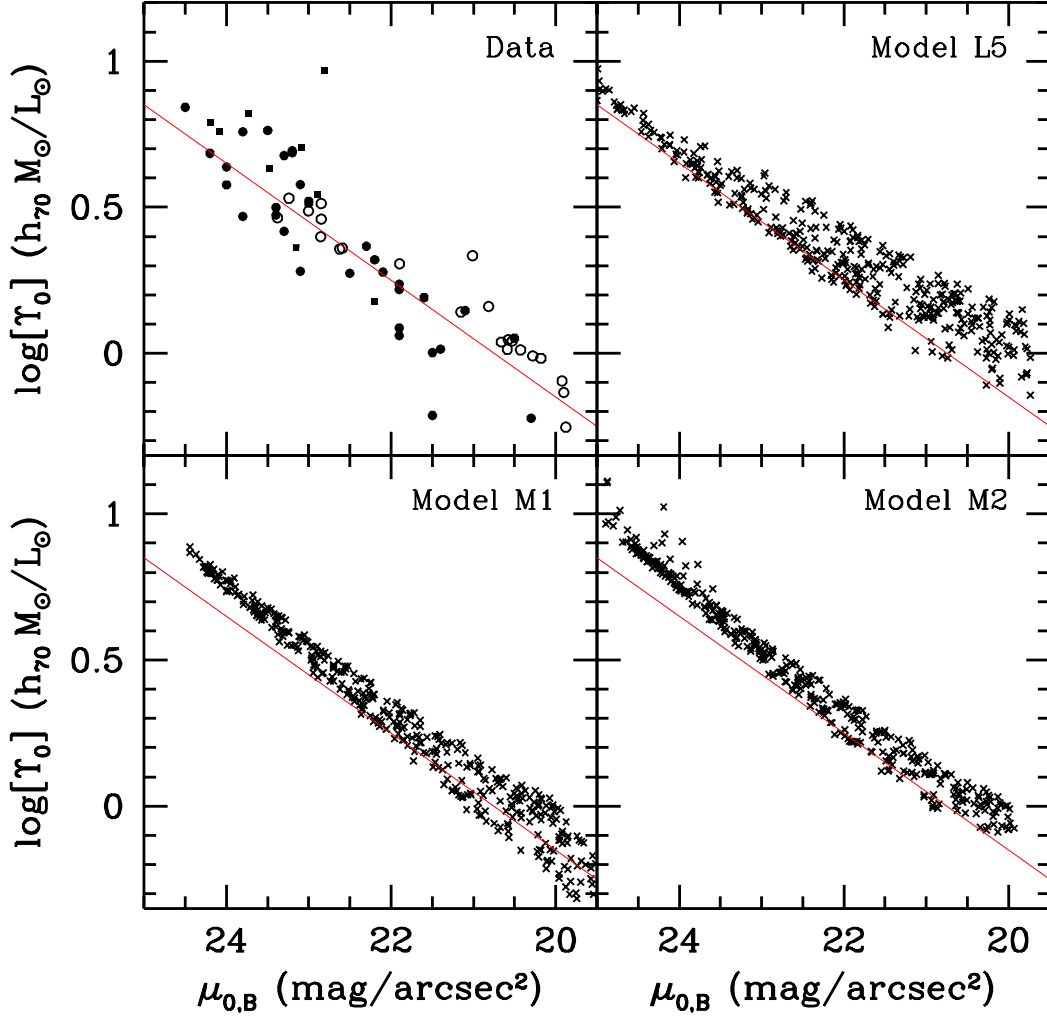


FIG. 6.— Same as Figure 4, except that we now plot the characteristic mass-to-light ratio Υ_0 as function of the disk's B -band central surface brightness $\mu_{0,B}$. The data reveal a narrow correlation, which is extremely well reproduced by each of the three models. The thin solid line corresponds to $\Upsilon_0^2 \Sigma_0^* = \text{constant}$, and is plotted with arbitrary normalization. See text for a detailed discussion.

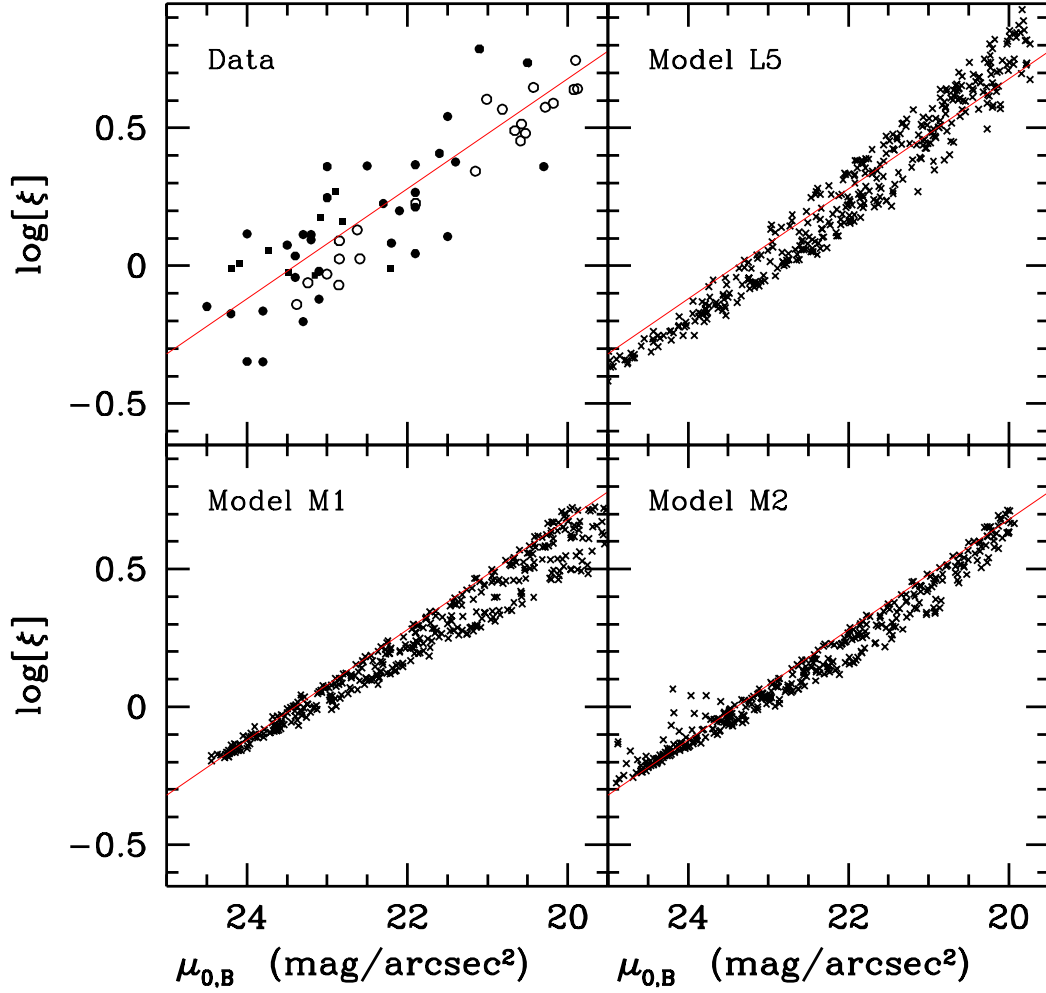


FIG. 7.— The characteristic acceleration ξ (see equation [13]) as function of central surface brightness $\mu_{0,B}$. The data and each of the three models reveal a narrow correlation, consistent with $\xi \propto \Sigma_0^{1/2}$ (the thin solid lines, plotted with arbitrary normalization). The origin of this relation is discussed in Appendix B.

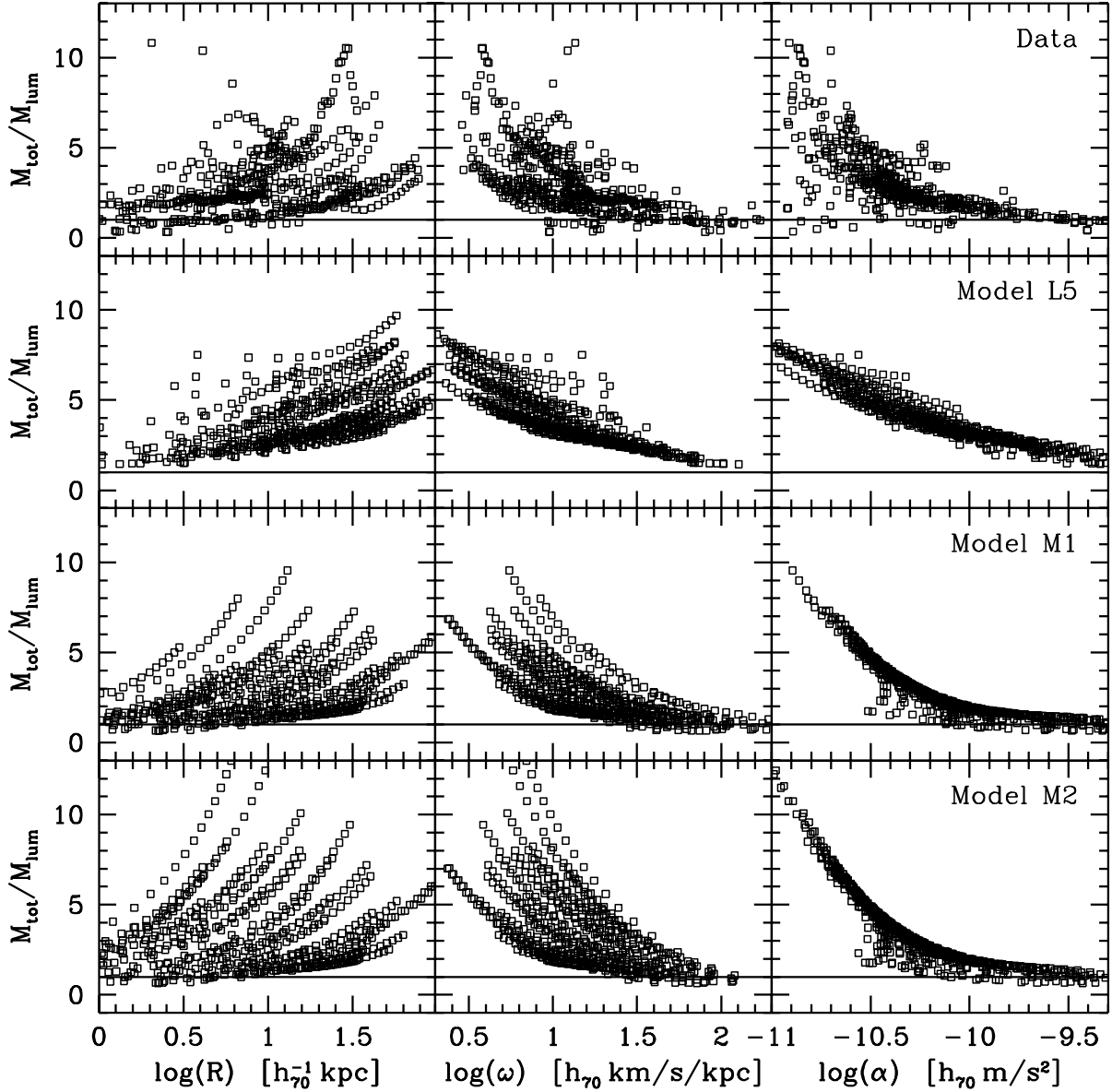


FIG. 8.— The ratio of total to luminous mass, $\Upsilon(R)$ (equation [14]), as function of radius R (panels on the left), orbital frequency ω (middle panels), and centripetal acceleration α (panels on the right). The upper panels plot the data for thirty galaxies from McGaugh (1998). These clearly reveal that the amount of scatter in Υ is minimized when plotted versus α , therewith indicating the presence of a characteristic acceleration. This character of the data is extremely well reproduced by the models. Whereas this is not surprising for the MOND models (M1 and M2), it is a remarkable success for the DM model.

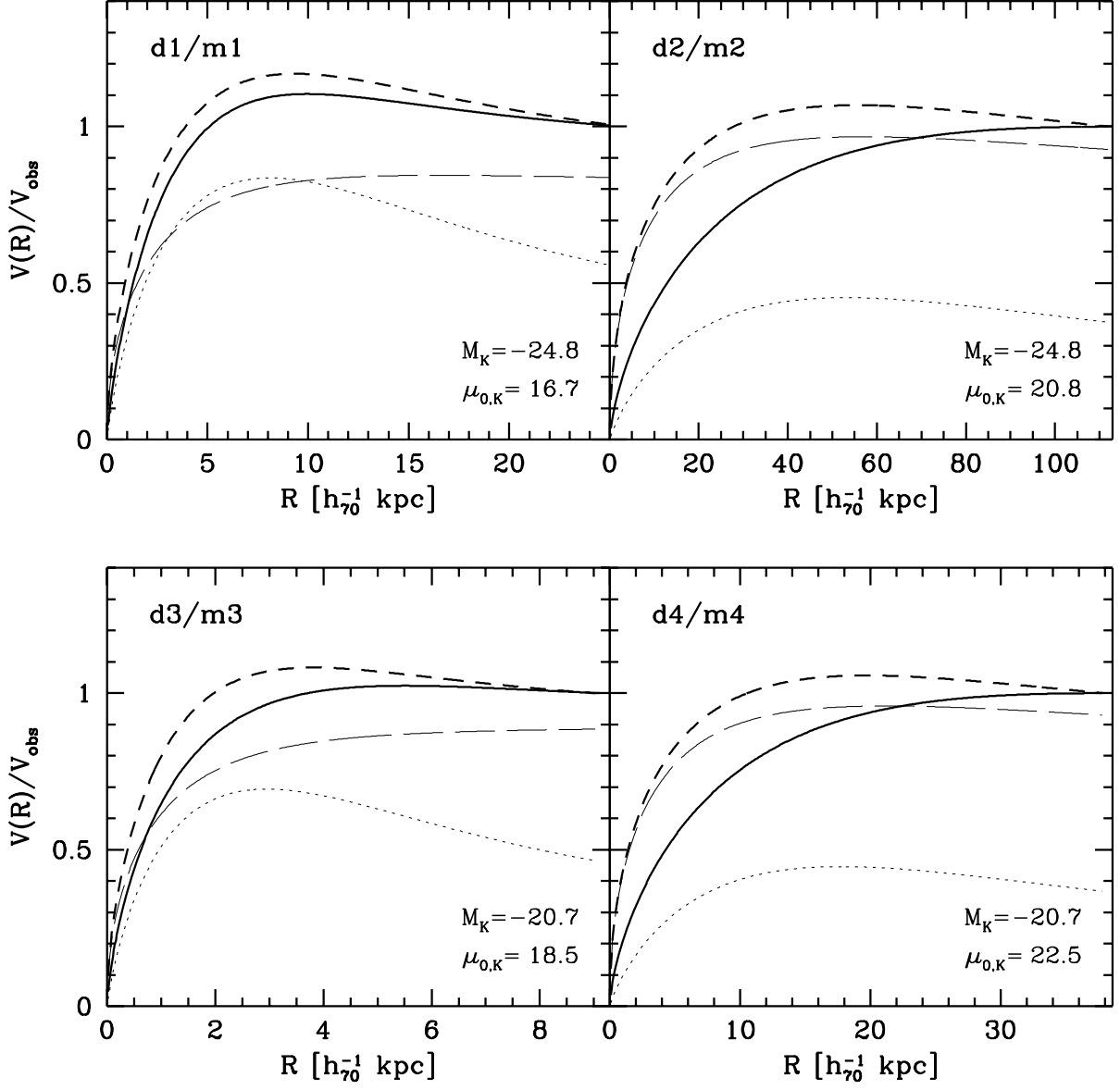


FIG. 9.— Rotation curves for model galaxies plotted up to the radius at which the HI column density reaches 10^{20} cm^{-2} . Thick solid lines correspond to the galaxies from model M1 (MOND), whereas the thick dashed lines are the rotation curves for galaxies from model L5 (CDM). The thin dotted lines and long-dashed lines correspond to the contributions from the disk and the dark halo, respectively. Each panel compares the rotation curves of two galaxies that have virtually identical photometric properties (see Table 2), and which are indicated in each panel. The four sets of galaxies span four magnitudes in both luminosity and surface brightness. Note that the difference between the DM rotation curves and those for MOND increase with decreasing surface brightness.

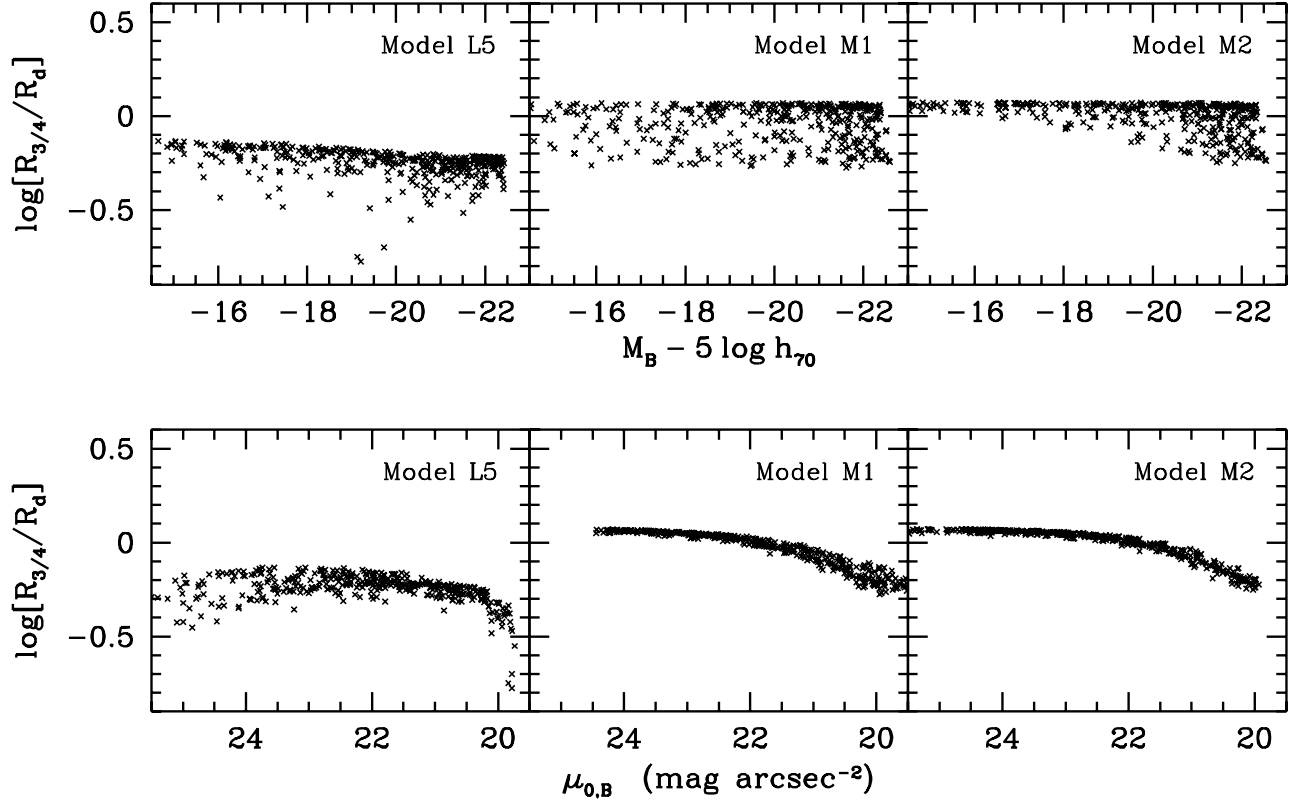


FIG. 10.— The ratio of $R_{3/4}$, defined as the radius where the RC reaches a velocity 75 percent of V_{flat} , to the disk scale length R_d as function of absolute B -band magnitude (upper panels) and central B -band surface brightness (lower panels) for each of the three models. Rotation curves in MOND are shallower (i.e., larger $R_{3/4}/R_d$) than in the case of DM, but only marginally so. Note that there is only a very marginal increase of $R_{3/4}/R_d$ with decreasing luminosity and surface brightness, in clear contradiction with the data presented in MB98a. In addition, both the DM and the MOND models, reveal a clear upper limit of $R_{3/4} \lesssim 0.8R_d$ and $R_{3/4} \lesssim 1.25R_d$ respectively. This again is in clear contrast to the data, which shows galaxies with $R_{3/4}/R_d$ as high as 3. The most likely explanation for this inconsistency seems that the data have not been properly corrected for beam-smearing (see discussion in text).

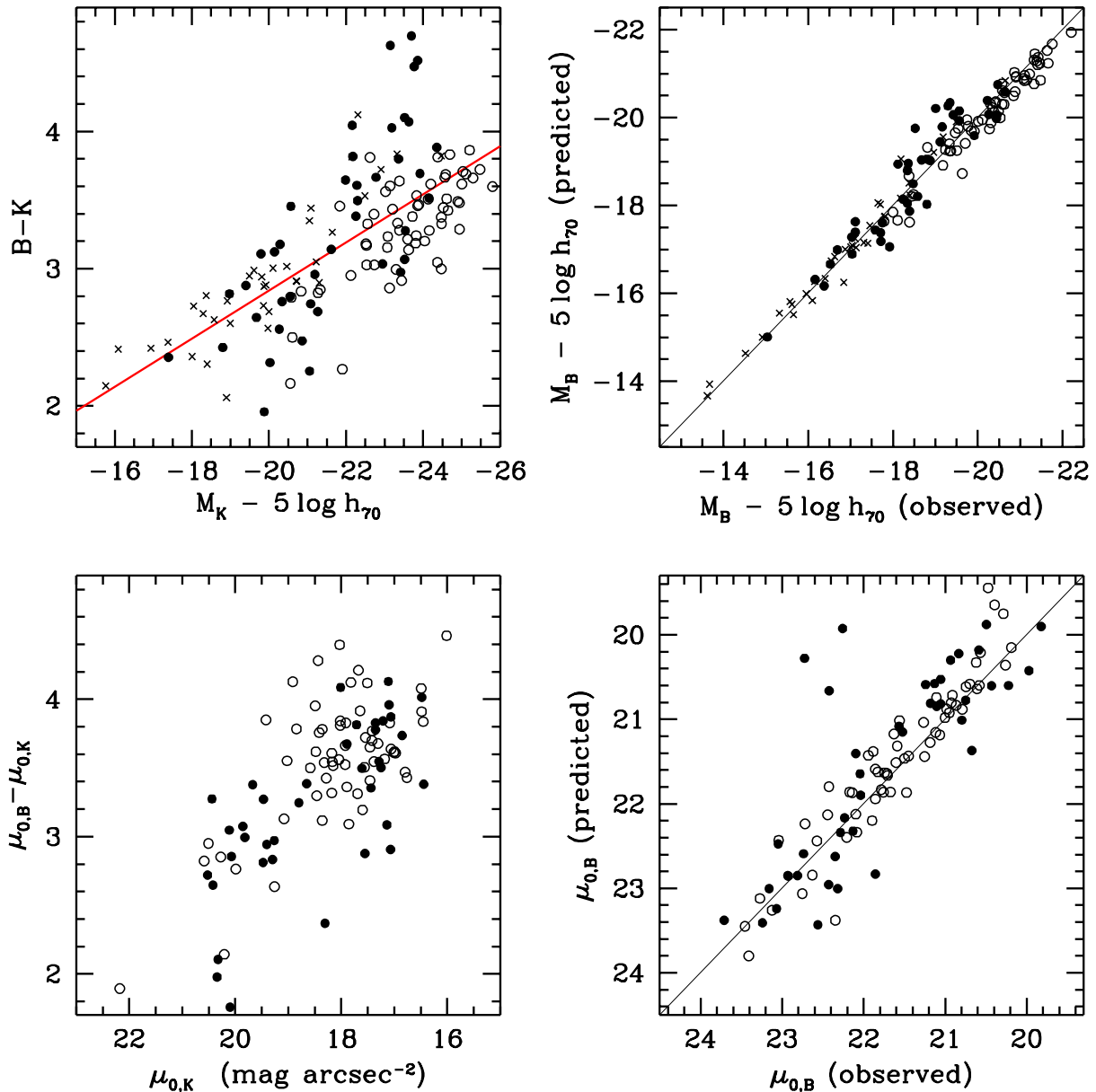


FIG. 11.— The upper left panel plots $B - K$ colors versus absolute K -band magnitude for an ensemble of disk galaxies. Data is taken from Verheijen (1997; solid circles), de Jong & van der Kruit (1994; open circles), and Dalcanton et al. (1999; crosses). All galaxies have been converted to a common distance scale with $H_0 = 70 \text{ km s}^{-1} \text{ Mpc}^{-1}$ and have been corrected for external extinction in a consistent way, using the reddening maps of Schlegel et al. (1998). No correction for internal extinction has been applied to the data. The thick solid line in the upper left panel is the best-fit linear color magnitude relation (equation [A1]). The upper right panel plots the predicted B -band magnitudes (based on the observed K -band magnitude and the best fitting $B - K$ color magnitude relation) versus the observed values. The agreement is reasonable with a standard deviation around the line $M_B^{\text{pred}} = M_B^{\text{obs}}$ (thin line) of 0.37 mag. The lower two panels plot similar figures, but for the central surface brightnesses, rather than the absolute magnitudes (see Appendix A for further details).

TABLE 1
PARAMETERS OF MODELS DISCUSSED IN THE TEXT.

ID. (1)	Hypothesis (2)	Q (3)	Υ_K^* (4)	$\varepsilon_{\text{SN}}^0$ (5)	ν (6)	b (7)	σ_M (8)
L5	CDM	1.5	0.40	0.05	-0.3	-10.5	0.20
M1	MOND	1.5	0.53	0.0	0.0	-10.6	0.21
M2	MOND	1.5	0.53	0.05	-3.0	-11.9	0.33

NOTE.—Column (1) lists the model ID, by which we refer to it in the text. Column (2) indicates whether the model is based on the DM or the MOND hypothesis. Columns (3) and (4) list the value of the Toomre parameter, Q , and the stellar K -band mass-to-light ratio in $h_{70} M_{\odot}/L_{\odot}$. Columns (5) and (6) list the feedback parameters $\varepsilon_{\text{SN}}^0$ and ν , respectively. Finally, columns (7) and (8) list the slope b and scatter σ_M (in mag) of the best fitting TF relation for model galaxies with $-19 \geq M_K - 5 \log h \geq -24$

TABLE 2
PARAMETERS OF MODEL GALAXIES DISCUSSED IN THE TEXT.

ID.	Model	M_K mag	R_d h_{70}^{-1} kpc	$\mu_{0,K}$ mag arcsec $^{-2}$	V_{flat} km s $^{-1}$	$R_{3/4}/R_d$	λ	c
(1)	(2)	(3)	(4)	(5)	(6)	(7)	(8)	(9)
d1	L5	−24.8	3.8	16.7	237.5	0.52	0.040	8.5
m1	M1	−24.8	3.8	16.7	216.2	0.68	—	—
d2	L5	−24.8	24.7	20.8	213.9	0.41	0.179	8.3
m2	M1	−24.8	25.0	20.8	233.8	1.17	—	—
d3	L5	−20.7	1.4	18.5	92.1	0.63	0.030	9.4
m3	M1	−20.7	1.4	18.6	90.8	0.98	—	—
d4	L5	−20.7	8.3	22.4	97.1	0.46	0.144	9.8
m4	M1	−20.7	8.3	22.5	114.9	1.19	—	—

NOTE.—Column (1) lists the model galaxy ID, by which we refer to it in the text. Column (2) indicates the model on which the galaxy is based. Columns (3)-(5) list the K -band magnitude, M_K , the disk scale-length, R_d , and the central surface brightness, $\mu_{0,K}$, of the model galaxies, respectively. Column (6) lists the rotation velocities measured at a column density of $N[\text{HI}] = 10^{20} \text{cm}^{-2}$. The ratio of $R_{3/4}$ to R_d is listed in column (7). Finally, columns (8) and (9) list the spin parameter λ , and the concentration parameter c of the NFW halo profile (before adiabatic contraction). Since we only use these parameters in the DM models, no values are listed for the MOND galaxies. All values listed correspond to $h_{70} = 1$

TABLE 3
RESULTS.

Observation (1)	item (2)	figure (3)	L5 (4)	M1 (5)	M2 (6)
near-IR TF relation	1	1	+	+	-
M_{HI}/L_B	4	2,3	+	+	+
Υ_0 vs. M_B	3	4	+	-	+
Υ_0 vs. $\mu_{0,B}$	3	6	+	+	+
$\mu_{0,B}$ vs. V_{flat}	-	5	+	-	+
ξ vs. $\mu_{0,B}$	-	7	+	+	+
$\Upsilon(R, \omega, \alpha)$	6	8	+/-	+	+
RC shapes	2	9,10	+/-?	+?	+?

NOTE.—Column (1) indicates the observational constraint. Columns (2) and (3) refer to the item number of the list of observational facts presented in §1, and to the number of the figure in which a comparison of the models with the data is presented. Columns (4) to (6) indicate whether each of the three models discussed in this paper are consistent (+), inconsistent (-), or only marginally consistent (+/-) with the data. A question mark indicates that more data and/or work is needed before a definite answer can be given.